Journal of Biogeography

WILEY

Journal of Biogeography

RESEARCH ARTICLE OPEN ACCESS

Diel Vertical Migration Shapes North Atlantic Copepod Bioregions

Marion Vilain[1] | Eric Goberville[2] | Dorothée Vincent[3] | Fabio Benedetti[4] | Frédéric Olivier[2,5]

[1]Sorbonne Université, CNRS, Laboratoire d'Océanographie de Villefanche, LOV, Villefranche-sur-Mer, France | [2]Laboratoire de Biologie des Organismes et des Ecosystèmes Aquatiques–BOREA, Muséum National d'Histoire Naturelle (MNHN), SU, CNRS, IRD, UA, Paris, France | [3]PatriNat (OFB, MNHN), Brest, France | [4]Institute of Plant Sciences, University of Bern, Bern, Switzerland | [5]Université Bretagne Occidentale (UBO), CNRS, IRD, Institut Universitaire Européen de la Mer, Plouzané, France

Correspondence: Marion Vilain (marion.vilain@imev-mer.fr; marion.vilain@protonmail.com)

Received: 31 May 2024 | **Revised:** 27 February 2025 | **Accepted:** 3 March 2025

Keywords: biogeography | Continuous Plankton Recorder | copepod communities | DVM | functional traits | network clustering | zooplankton macroecology

ABSTRACT

Aim: Assessing the influence of diel vertical migration (DVM) on biogeographic patterns to improve the macroecological characterisation of the structure and function of zooplankton communities.

Location: North Atlantic Ocean and adjacent seas.

Taxon: Marine copepod species.

Methods: We base our bioregionalisation on Continuous Plankton Recorder (CPR) data of copepod species abundances from 1966 to 2021. We separate day and night samples using the solar elevation corresponding to civil twilight. For each condition, we interpolate abundances onto a grid adapted to the irregular sampling effort. We then generate a bipartite network (geographical cells—species) on which we apply the Map Equation clustering algorithm to delineate bioregions and identify their underlying copepod communities. We use canonical correspondence analyses to characterise the resulting bioregions in terms of environmental forcings, species composition and community-weighted mean traits.

Results: We identify four bioregions for both day and night partitions, with dynamic transitions and changes in spatial patterns as well as in community composition between day and night. While environmental forcings seem to transcend diel variations, ecological features of bioregions show day/night discrepancies: higher copepod diversity at night is driven by changes in species composition mediated by diel vertical migration.

Main Conclusions: We highlight how day/night variations driven by highly migratory copepod species shape community spatial patterns and species composition. We uncover distinct levels of functional diversity across bioregions, suggesting different responses of copepod communities to environmental changes. Transition zones emerge as crucial markers of pelagic bioregion connectivity, emphasising their dynamic nature. Embracing a partitioning approach that better captures these dynamics is essential for understanding how ecosystems function and will evolve in response to climate changes.

1 | Introduction

Historically, studies in ocean biogeography have relied on physical predictors of species distribution, such as surface temperature or global circulation (Reygondeau and Dunn 2019), to overcome the scarcity and limited availability of biological observations (Ratnarajah et al. 2023). This assumes that biological communities strongly respond to environmental variations (Boudinot and Wilson 2020). Although these predictors are effective in ecosystems with marked transitions such as foreshore benthic habitats

(Lewis 1964), their applicability in the pelagic realm is less clear due to the widespread dispersal of communities driven by strong water mass connectivity. Recently, Beaugrand et al. (2019) combined phytoplankton and zooplankton richness estimates with habitat characteristics to define an ecological partition of the North Atlantic Ocean and its adjacent seas. While this partition captures habitat physical features, it only partially describes the biotic composition within ecological units, a critical aspect for deciphering the underlying community structure governing biogeographic patterns (Pata et al. 2022). Kléparski et al. (2021) extended this work by linking the environmental signatures of phytoplankton and zooplankton assemblages to the ecological partition defined by Beaugrand et al. (2019). The dominant patterns among previous North Atlantic partitioning reflect large-scale oceanographic features, such as the Polar Front and the Gulf Stream extension, resulting in a clear oceanic/neritic distinction along a latitudinal gradient from colder to warmer waters. Historical data from the North Sea reveal that rising temperatures in the 1980s facilitated the replacement of cold-water by warmer-water species, some expanding their range northwards by over 10° to track their thermal optima (Beaugrand 2004; Beaugrand and Ibanez 2004). Warmer-water species generally have lower energy-rich lipid content than cold-water species (Cavallo and Peck 2020), which can negatively impact the food intake and survival of larvae from higher trophic levels (Record et al. 2018). This suggests that looking into species traits makes it possible to characterise certain community functions and thus provide a mechanistic understanding of potential ecological consequences of biogeographic shifts (Violle et al. 2007).

Increasingly adopted in marine macroecology (Barton et al. 2013), trait-based approaches focus on key traits—interrelated through trade-offs—influencing the fitness of a species in a given environment (Litchman et al. 2013). Studying traits—common to all life forms—helps overcome taxonomic complexity by relying on a comparable unit (Hébert and Beisner 2020). McGinty et al. (2018) showed that copepod traits (body size, dietary and life history strategies) may partially determine their realised niches, emphasising the significance of trait-based analyses in understanding species distributions. Benedetti et al. (2023) highlighted a pronounced latitudinal gradient in copepod functional traits expression—including body size, trophic group, dietary strategy, myelination and spawning mode—driven by global abiotic gradients such as temperature. This latitudinal gradient is particularly evident for body size (e.g., Bergmann 1848), a key trait influencing vital processes (e.g., growth, fecundity, metabolism; Barton et al. 2013) as well as prey–predator interactions (Munk 1997). This in turn influences ecological processes and ecosystem functions. For instance, large and intermediate-sized copepods contribute more to carbon cycling than smaller copepods (Stamieszkin et al. 2015) by producing larger, faster-sinking faecal pellets (i.e., which spend less time in the water column and are therefore less degraded; Turner 2002), and by respectively living deeper in the water column and performing diel vertical migrations (i.e., respiration and excretion at greater depths; Bandara et al. 2021; Ohman and Romagnan 2016).

Diel vertical migration (DVM) is a particularly striking behavioural trait in allegedly passive drifters, which describes how some species can migrate to different depths in the water column throughout the day, with amplitudes that can reach hundreds of metres (Conroy et al. 2020). This complex mechanism is controlled by both exogenous (e.g., irradiance, temperature-linked water stratification) and endogenous (e.g., circadian rhythm) cues (Bandara et al. 2021). DVM can be seen as a trade-off between feeding opportunities in food-rich near-surface waters and predator avoidance (Ohman 1990; Thygesen and Patterson 2019), which can lead to cascading DVMs through food webs (Bollens et al. 2011). DVM influences several features of zooplankton life, including dampening UV radiation exposure (Williamson et al. 2011) and optimising dispersal (Batchelder et al. 2002). Synchronised vertical movements of metazoans can transport particulate matter across density gradients (Katija and Dabiri 2009) and consequently play an essential role in the biological carbon pump, with an estimated contribution of more than 50% of the global total of carbon sequestered by the biological pump (Pinti et al. 2023). Therefore, DVM tightly links ecological and biogeochemical processes. Yet its impact on marine zooplankton biogeography remains poorly understood. While some regional DVM-related variations in diversity patterns of calanoid copepods have been described (Beaugrand et al. 2001), the influence of DVM on large-scale biogeographic patterns remains understudied (Brun et al. 2016)—partly because of the challenging need for data with good horizontal and taxonomic resolutions combined with a day/night sampling—and is often overlooked in functional approaches (Becker et al. 2021; Benedetti et al. 2023; Djeghri et al. 2023). Here, we partition the North Atlantic Ocean using a network approach based on copepod abundances to demonstrate the influence of DVM on the composition and spatial distribution of marine zooplankton communities, with the aim of better integrating the role of vertical processes of pelagic connectivity.

2 | Materials and Methods

The different steps of this study are synthesised in Figure 1. All analyses were performed using R Statistical Software (v4.3.2; R Core Team 2023).

2.1 | Delineation of Bioregions Based on Copepod Species Abundance

2.1.1 | Continuous Plankton Recorder Data

This study investigates zooplankton communities in the North Atlantic Ocean and its adjacent seas, spanning from 80°W to 30°W longitude and 25°N to 80°N latitude. We used data from the Continuous Plankton Recorder (CPR) Survey, a long-standing monitoring programme managed by the Marine Biological Association of the UK (MBA, 2022). Plankton samples are routinely collected by the CPR, a sampling instrument towed through the surface layer of the ocean (~5–10 m deep). While CPR data cannot fully depict the water column, Hélaouët et al. (2016) demonstrated their reliability compared to vertical trawl samples. The CPR allows seawater to flow through, filtering plankton with a 270 μm mesh silk band—which may lead to underestimating certain small taxa and plankton abundances (Lewis et al. 2006; Richardson et al. 2006)—before storing it in 4% formalin (Hardy 1939). Samples are identified to species, and

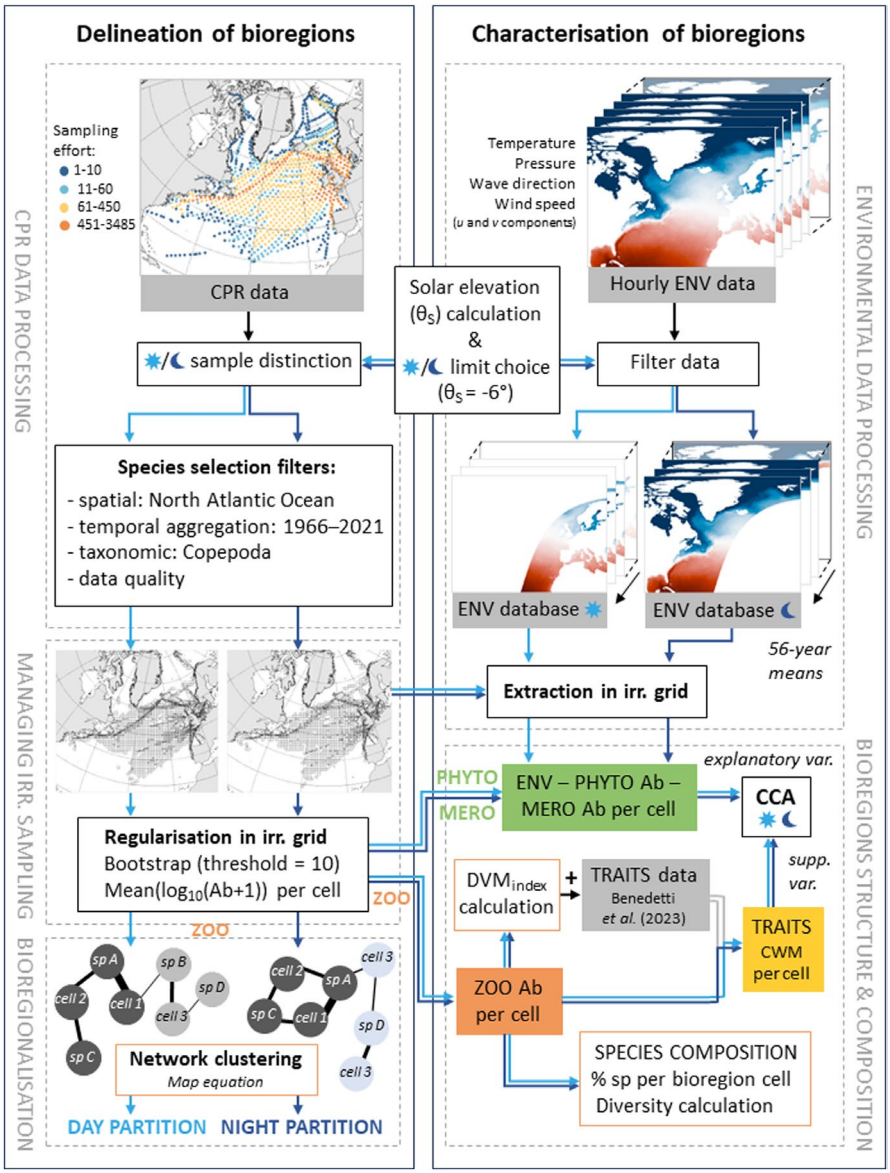

FIGURE 1 | Flow chart illustrating the key analyses conducted in this study. Each analysis is performed separately for day (light blue flow) and night (dark blue flow). Abbreviations: Ab, abundance; CCA, canonical correspondence analysis; cell, geographical cell; CPR, Continuous Plankton Recorder; CWM, community-weighted means; DVM, diel vertical migration; ENV, environment; irr., irregular; MERO, meroplankton (fish larvae and invertebrate larvae); nb, number; PHYTO, phytoplankton (diatoms and dinoflagellates); sp., species; supp., supplementary; var., variable; ZOO, zooplankton.

semi-quantitative abundances are estimated (Batten et al. 2003). Sampling methods and analysis procedures have remained consistent since 1958 (Reid et al. 2003).

2.1.2 | Species Selection

We applied both taxonomic and robustness filters to ensure high-quality zooplankton data identified at the species level. We focused on adult copepods as species-level data predominantly represent this class and life stage. The CPR database exhibits a gradual increase in the number of species identified over time that reflects not only the advancement of taxonomic knowledge but also the introduction of new species. To ensure consistent tracking of the same species over an extended period, we selected the 1965 taxonomic dataset (MBA, 2022). This approach offers a consistent long-term perspective on species community changes while maximising the inclusion of diverse species. Consequently, this study covers the period 1966–2021. It should be noted that the successive taxonomic filters induce an underestimation of the real variability in species composition and exclusively reflect Calanoid (96%) and Harpacticoid (4%) copepods, excluding dominant Cyclopoid genera such as *Corycaeus, Oithona*, and *Oncaea,* and some abundant Calanoid genera such as *Calocalanus* and *Clausocalanus*.

2.1.3 | Day/Night Distinction

To integrate the effects of diel variations on copepod community composition and abundance into the delineation of bioregions, we separated day and night samples using three solar elevation (θ_s)

thresholds: the civil ($\theta_s = -6°$), nautical ($\theta_s = -12°$) and astronomical twilight ($\theta_s = -18°$). Bioregions remained consistent across scenarios (Appendix Figure S1), so we retained the civil twilight scenario as it offered the most balanced day/night ratio. The resulting dataset comprises 125,107 day samples and 93,498 night samples, encompassing 72 and 77 copepod species, respectively.

2.1.4 | Dealing With Irregular Sampling: Regularisation of CPR Data

To mitigate the effects of sampling heterogeneity and improve the detection of the signal-to-noise ratio associated with spatial dynamics within copepod communities (Goberville et al. 2014), we set up two grids (one for day, one for night) adapted to the sampling effort using a quadtree approach (*AQuadtree* R package v1.0.4; Lagonigro et al. 2023). Geographical cell sizes are adjusted to incorporate a minimum of 10 observations: areas with a high sampling density (e.g., in the North Sea) display smaller cells than regions with lower sampling density (e.g., off the North Atlantic). Within each geographical cell, we resampled abundances with a minimum of 10 observations per cell and 999 permutations. Zero abundances were treated as true absences and were also resampled to ensure unbiased representation across grid cells. The seasonal distribution of CPR samples and spatial coverage being consistent year-round (Appendix Figure S2), we were able to calculate the 56-year average of $\log_{10}$(abundance+1) for each species, resulting in a biological matrix in the format [Site×Species×Abundance], for both day and night. Given the semi-quantitative nature of CPR data, the log-transformation produces clearer and more representative biogeographic patterns (see Appendix Figure S3 for a comparison of log-transformed vs. untransformed abundances).

2.1.5 | Bioregionalisation Using Network Clustering

To map day/night bioregions, we applied a biogeographic network approach (Leroy et al. 2019; Vilhena and Antonelli 2015), using the R package *biogeonetworks* (v0.1.2; Leroy 2024) on each [Site × Species × Abundance] matrix. This approach involves generating a bipartite network composed of *(i)* geographical cells and *(ii)* species, forming a set of nodes interconnected by links: when a species is present in a geographical cell, a link is established between species and cell, and the link is weighted by the associated abundance value. To delineate bioregions, we applied the Map Equation hierarchical clustering algorithm (Rosvall and Bergstrom 2008) on this network, which groups nodes into clusters based on high intra-group and low inter-group connectivity. In other words, the algorithm creates groups of cells that share the same species with similar abundance patterns. In practice, it relies on information theory: it measures the per-step average length of binary code needed to describe the movements of a random walker on the network and find the partition that minimises the total length (L) of this description. The Map Equation algorithm has been widely recommended for identifying biogeographic regions (Bloomfield et al. 2018; Edler et al. 2016; Leroy et al. 2019; Rojas et al. 2017; Vilhena and Antonelli 2015) and has found applications in diverse fields such as disease-related insect distribution (e.g., Ferrari et al. 2022), change in biogeographic patterns due to human activities (e.g., Leroy et al. 2023) and benthic biogeographies (e.g., Victorero et al. 2023; Watling and Lapointe 2022). Because Map Equation is a stochastic algorithm, it was iterated 1000 times to let it converge towards an optimal solution, enhancing the robustness of the analysis and mitigating potential variations induced by minor changes in the data or parameters. Additionally, we computed two clustering metrics: the codelength of a node reflects its importance in the overall connectivity of the network (Bohlin et al. 2014): the higher its value, the most structuring the node is in the network; the participation coefficient measures the connectivity across clusters: higher values reflect a greater number of links a node has to different regions (Bloomfield et al. 2018). For a geographical cell, the participation coefficient indicates whether it contains species from other regions (i.e., transition zones; Victorero et al. 2023). The present bioregions represent a snapshot at 10 m depth, which biases the observed patterns of species dominance towards surface-dwelling species. Larger species, such as *Heterorhabdus norvegicus* (Yamaguchi et al. 2022), typically inhabit deeper layers of the water column and are likely underrepresented in our dataset.

2.2 | Environmental and Ecological Characterisation of Bioregions

2.2.1 | Environmental Variables

Hydro-climatic and atmospheric hourly ERA5 data from 1966 to 2021 were retrieved from the Copernicus Climate Change Service (Hersbach et al. 2023). The spatial resolution for atmospheric parameters—including sea surface skin temperature (K), mean sea level pressure (Pa) and wind (10 m *u*- and *v*-component; m s^{-1})—is 0.25°×0.25°, while for mean ocean wave direction (degree true) it is 0.5°×0.5°. Sea surface skin temperature serves as a reliable proxy for downward irradiance and exhibits a strong diel cycle signature. Bathymetry (m) was extracted from the General Bathymetric Chart of the Oceans (GEBCO Compilation Group 2022), with a spatial resolution of 15 arc sec. We calculated the solar elevation at the scale of the North Atlantic Ocean between 1966 and 2021 using the *SolarAzEl* Matlab function (v1.1.0.0; Koblick 2023), which we translated into R language. Using the civil twilight as the day/night limit ($\theta_s = -6°$), we generated binary filters to segregate environmental datasets for day and night conditions. We computed 56-year means, alongside standard deviations (σ), of each environmental variable for both day and night.

2.2.2 | Ecological Covariates

Phytoplankton and meroplankton data (cells L^{-1}) were extracted from the CPR dataset (MBA, 2022). Phytoplankton taxa were categorised into dinoflagellates and diatoms. Meroplankton was divided into fish larvae and invertebrate larvae. This taxonomic partitioning was chosen because of their contrasting trophic roles within marine ecosystems. Diatoms form the base of the copepod–fish food web, providing significant nutritional value, while dinoflagellates offer lower nutritional benefits (McQuatters-Gollop et al. 2007). Fish larvae often prey upon small copepods and their nauplii (Turner 2004), while larvae of many benthic invertebrate species have minimal effects on

their food supply due to their relative scarcity compared to potential competitors (Strathmann 1996). Invertebrate young stages include *Lepas* nauplii, Bivalvia, Decapoda, cirripede and polychaete larvae, echinoderm larvae and post-larvae. Day and night samples were differentiated and abundances were transformed into $\log_{10}$(abundance+1) and regularised using the same methodology described for copepod communities.

2.2.3 | Species Traits

Five traits (body size, myelination, feeding mode, trophic group and spawning strategy) were extracted from Benedetti et al. (2023) for 71 of the 78 copepod species of our CPR dataset (Figure 2). Missing body size data were filled in according to Razouls et al. (2005–2024) for *Euchaeta pubera*, *Euchirella curticauda*, *Euchirella pulchra*, and *Paraeuchaeta tonsa* but remained unavailable for *Diaixis hibernica*, *Diaixis pygmaea*, and *Scottocalanus persecans*. We also computed a diel vertical migration index (DVM_{index}), following Equation (1). As bioregions are abundance-based, we used the day/night difference in species abundance over the study period as the basis for this index, contrasting with the biomass-based DVM estimate of Brun et al. (2019).

$$DVM_{index} = \frac{Ab_{Day} - Ab_{Night}}{Ab_{Day} + Ab_{Night}} \quad (1)$$

Ab_{Day} and Ab_{Night} represent the abundance of the species (ind. m^{-3}) during the day and night, respectively. This index was categorised according to its sign: $DVM_{index} < 0$ (i.e., more surface abundance at night) was classified as 'classic DVM', whereas $DVM_{index} \geq 0$ (i.e., more surface abundance during the day) was classified as 'reverse DVM'. Absolute values were used as relative proxies for DVM amplitude, with values ≥ 0.5 indicating strong DVM. Lowest DVM_{index} values observed in the day and night bioregions are referred to as 'minimal' and serve as a baseline. Intermediate values between these two thresholds are termed 'moderate'. Given the spatio-temporal variability of DVM (Irigoien et al. 2004), it should be noted that this index reflects long-term regional averages and cannot be generalised as the typical behaviour of a species. Community-weighted mean traits (CWM; Bruelheide et al. 2018), representing the 'typical' trait values of a community, were calculated using the *cwm* function of the *weimea* R package (v0.1.19; Zelený 2021).

2.2.4 | Analyses of the Spatial Structure and Species Composition of Bioregions

To assess how environmental and ecological variables (phytoplankton and meroplankton abundances) structure each bioregion, we performed two Canonical Correspondence Analyses (CCA) using the *cca* function from the *vegan* R package (v2.6.4; Oksanen et al. 2022). Pseudo *F*-ratios were determined to assess

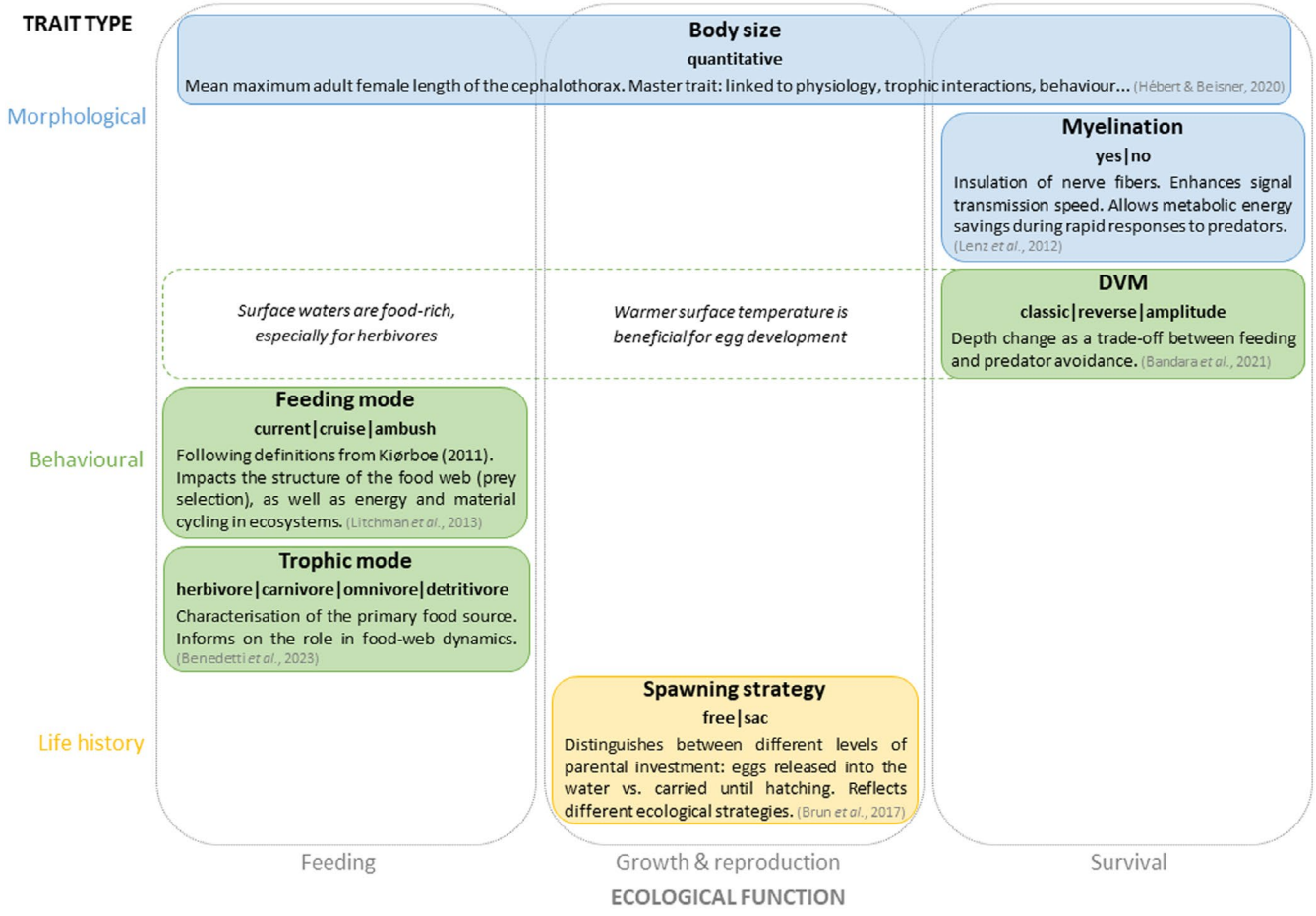

FIGURE 2 | Description of copepod traits used in this study and classified according to ecological function and type, following the framework of Litchman et al. (2013). Dotted lines indicate traits that may be of secondary importance for other functions.

the significance of constraints in the CCAs, using a permutation test with 999 permutations, implemented in the *anova.cca* function from the same package. Both CCAs showed significant results ($F = 32.764$, $p < 0.001$ for day; $F = 53.279$, $p < 0.001$ for night), with all explanatory variables being significant for the first two axes ($p < 0.001$).

Community-weighted mean trait values were projected as supplementary variables using the *envfit_cwm* function from the *weimea* R package. A test based on permuting species attributes (Zelený and Schaffers 2012) assessed the strength of relationships between CWM supplementary variables and ordination axes. It considers that species abundances are used both to build CCA axes and to compute CWM, preventing an overestimation in relationship strength (Zelený 2018). With 999 permutations, no significant correlation was found ($p > 0.1$), indicating that CWM can only be interpreted qualitatively, as illustrative variables (Figure 3c). To preserve geographical significance in line with bioregion mapping (Figure 3a), axis 1 is represented on the ordinate and axis 2 on the abscissa.

All variables were averaged by bioregions and statistically compared through Kruskal–Wallis tests followed by Dunn post hoc tests with Hochberg adjustment, respectively using the *kruskal_test* and *dunn_test* functions from the *rstatix* R package (v0.7.2; Kassambara 2023). Shannon's and Simpson's diversity indices were computed for copepod communities using the *diversity* function from the *vegan* R package.

Species compositions of each bioregion were summarised through boxplots representing the percentage of species abundance in their respective bioregions, calculated using Equation (2):

$$p_{x_i j} = \frac{Ab_{x_i j}}{\sum_{j=1}^{n} Ab_{x_i j}} \times 100 \quad (2)$$

Bioregion $X = \{x_i\}_{1 \le i \le m}$ is defined as the set of m geographical cells x_i. For any geographical cell x_i containing n total species affiliated to bioregion X, the abundance of species j is denoted $Ab_{x_i j}$. The percentage of abundance represented by species j in cell x_i is denoted $p_{x_i j}$.

3 | Results

3.1 | Spatial Structures of Bioregions and Their Variations Between Day and Night

Four significantly distinct bioregions (Kruskal–Wallis tests: $p < 0.001$), aggregated across the period 1966–2021, were delineated for both day and night conditions (Figure 3a). Two gradients emerge as key factors shaping the partitions. A latitudinal North–South gradient separates northern bioregions A and E from southern counterparts D and H. A longitudinal continental shelf–open ocean gradient extending from the Grand Banks of Newfoundland to the Northwest European continental shelf distinguishes bioregions B and F from the others. Day–night discrepancies in spatial patterns are particularly evident between continental shelf bioregions B and F. Bioregion F (night) covers a broader area since, in addition to the North Sea and European continental shelves (B), it encompasses the British Isles, Celtic seas, and Armorican continental shelves (eastern Atlantic). This pattern is mirrored in the western Atlantic, with the addition of the Georges Bank shelf to the Grand Banks of Newfoundland and the Scotian shelf (B). Bioregion G (night) has a more open ocean and northern distribution in the Northeast Atlantic than bioregion C. These specificities highlight dynamic transitions between bioregions, with overlapping boundaries and biogeographical cell exchanges between day and night (Figure 3b).

3.2 | Environmental and Ecological Factors Shaping Bioregions

Canonical Correspondence Analyses (CCA) allow us to characterise the environmental conditions and ecological distinctiveness of each bioregion (Figure 3c). Explanatory variables explain 32%|45% of the day–night variance in copepod species abundances, with the first two axes explaining 22.6%|29.4%. Bioregions are depicted as 95% confidence ellipses of sites distribution (assumed to be normal as species abundances are log-transformed) and their environmental characteristics are detailed in Table 1. The *y*-axis of the CCA (axis 1) highlights the latitudinal distribution of bioregions and is mostly structured by environmental variables, with sea surface skin temperature (correlation to axis: $r_{day} = -0.93$ and $r_{night} = -0.97$) and atmospheric pressure ($r_{day} = -0.88$; $r_{night} = -0.80$) as main drivers. It is also structured—to a lesser extent—by wave direction ($r_{day} = -0.54$; $r_{night} = -0.60$) and environmental variations (σ) in pressure ($r_{day} = 0.58$; $r_{night} = 0.33$), in wave ($r_{day} = 0.47$; $r_{night} = 0.29$), in eastward wind speed (σ_{U_WIND}; $r_{day} = 0.44$; $r_{night} = 0.31$) and in sea surface skin temperature ($r_{day} = 0.35$; $r_{night} = 0.42$). For night condition, bathymetry also exerts a moderate influence on axis 1 structuring ($r_{night} = 0.52$). The *x*-axis (axis 2) reflects a longitudinal pattern indicative of inshore influence. Main covariates in the positive part of axis 2 include invertebrate larvae abundance ($r_{day} = 0.76$; $r_{night} = 0.87$) and bathymetry ($r_{day} = 0.74$; $r_{night} = 0.66$), as well as fish larvae ($r_{day} = 0.56$; $r_{night} = 0.59$), dinoflagellate ($r_{day} = 0.56$; $r_{night} = 0.52$) and diatom ($r_{day} = 0.48$; $r_{night} = 0.37$) abundances. The negative part of this axis is associated with variations in wave direction ($r_{day} = -0.42$; $r_{night} = -0.58$), and for night condition, with variations in pressure ($r_{night} = -0.49$) and in eastward wind speed ($r_{night} = -0.44$).

The northernmost bioregions (A|E) are located in the positive part of axis 1, reflecting colder waters (7.8°C ± 0.2°C and 7.1°C ± 0.2°C on average, respectively) and relatively lower atmospheric pressure. These bioregions also experience stronger environmental variations (σ) in wave direction, wind speed, atmospheric pressure, and sea surface skin temperature. Located in the negative part of both axis 1 and axis 2, southern bioregions (D|H) are characterised by warmer temperatures (17.7°C ± 0.2°C |16.6°C ± 0.2°C) and encompass open-ocean waters ranging from depths of 1036–4928 m or 946–4860 m, respectively. They exhibit the lowest diatom abundances (23.1 ± 1.8 cells L^{-1}|19.2 ± 1.3 cells L^{-1}). Conversely, bioregions B and F, located in the positive part of axis 2, are predominantly influenced by high meroplankton and phytoplankton abundances (e.g., 263.3 ± 34.5 ind. m^{-3}|101.5 ± 8.7 ind. m^{-3} for invertebrate larvae), reflecting the vicinity of the coasts, with bioregion B

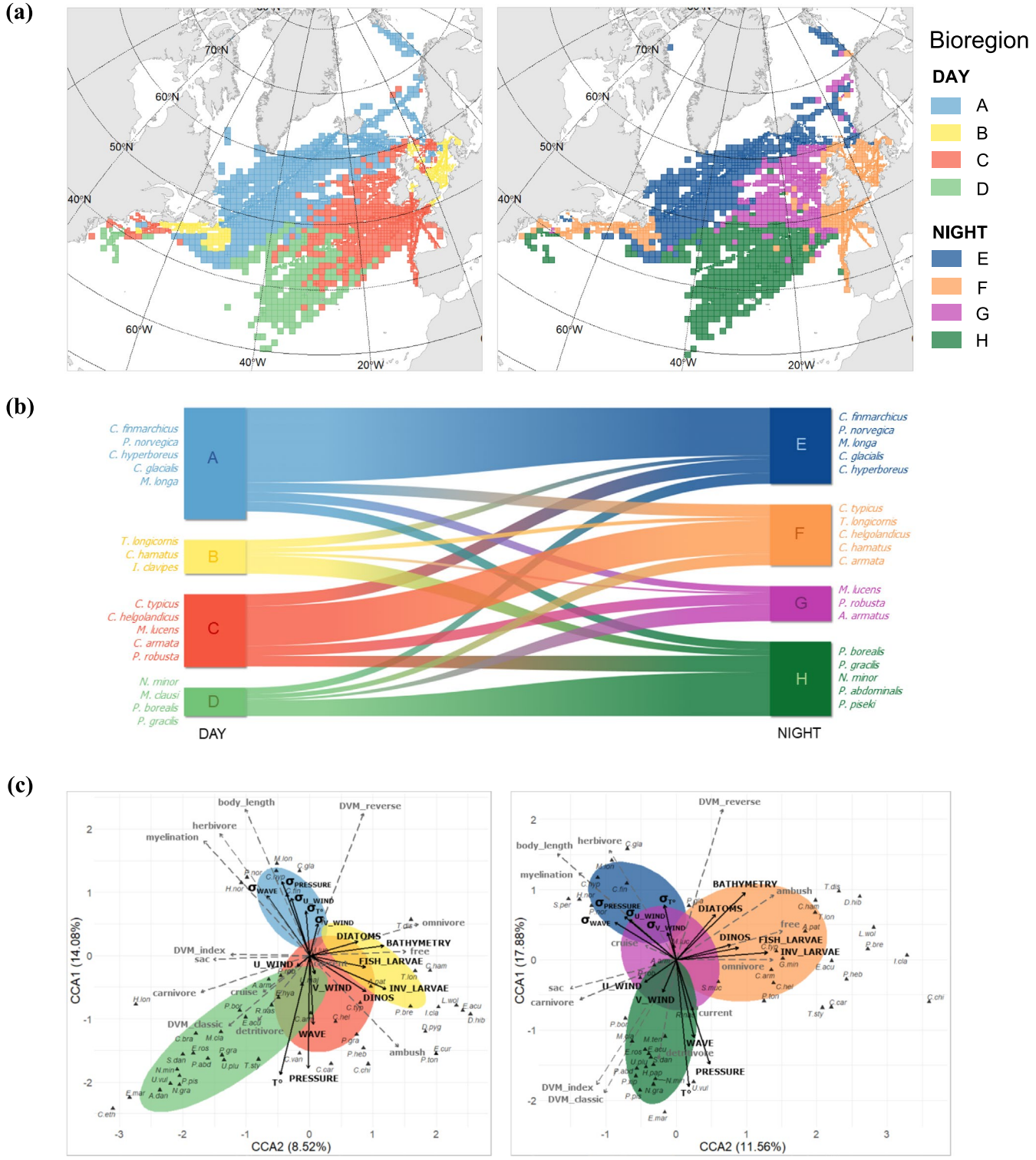

FIGURE 3 | Bioregions generated by network clustering with their fluxes between day and night and associated environmental and ecological characteristics. Different colours indicate different bioregions. (a) Copepod-based bioregions of the North Atlantic Ocean over the 1966–2021 period (scenario $\theta_s = -6°$) during day (left) and night (right) resulting from optimal partitions ($L_{DAY} = 7.10$ bits; $L_{NIGHT} = 7.66$ bits). Mapping in Equivalent Lambert azimuthal projection. (b) Alluvial diagram showing species and geographical cell fluxes between day and night bioregions. Only the first 3–5 most structuring species of each bioregion are represented. (c) Canonical correspondence analysis (CCA) on environmental and biological variables (scaling 1; solid black lines) during day (left) and night (right). The first 2 axes of the CCA are represented (axis 1 on the *y*-axis; axis 2 on the *x*-axis), and 95% confidence ellipses of the distribution of sites are drawn. Community-weighted mean traits (CWM) are added as supplementary variables (dotted grey lines). Only the first 17 most structuring species of each bioregion are represented (see Figure 4) and abbreviated using the first letter of the genera and the first three letters of the species (see Figure 4 for full names).

TABLE 1 | Characteristics of bioregions in terms of copepod structure and diversity, environmental conditions, and ecological composition including phytoplankton and meroplankton abundances as well as copepod community-weighted mean trait values (CWM; mean ± standard error).

	Bioregions							
	Day				Night			
	A	B	C	D	E	F	G	H
Copepod structure and diversity								
Species richness	53	45	66	62	55	68	55	69
Structuring species (%)	13.2	20.0	25.8	62.9	14.5	25.0	9.1	68.1
Zooplankton Ab (ind. m^{-3})	44.7 ± 1.8 (a)	141.5 ± 8.7 (b,c)	52.4 ± 5.6 (d)	11.5 ± 1.7 (e)	52.5 ± 2.4 (f)	119.4 ± 7.3 (b)	22.1 ± 1.4 (g)	20.0 ± 1.1 (c,f)
Shannon diversity index	0.4 ± 0.0 (a)	1.0 ± 0.0 (b)	0.9 ± 0.0 (c)	1.5 ± 0.0 (d)	0.7 ± 0.0 (b)	1.1 ± 0.0 (e)	1.4 ± 0.0 (d)	2.0 ± 0.0 (f)
Simpson diversity index	0.2 ± 0.0 (a)	0.5 ± 0.0 (b)	0.4 ± 0.0 (b)	0.6 ± 0.0 (c)	0.3 ± 0.0 (d)	0.5 ± 0.0 (e)	0.6 ± 0.0 (c)	0.8 ± 0.0.0 (f)
Environment								
Bathymetry (depth in m)	2366 ± 65	63 ± 29	2770 ± 95	3539 ± 66	2277 ± 75	105 ± 85	2751 ± 99	3665 ± 51
Median (max–min)	(64–4821) (a,b)	(20–2083) (c)	(28–4872) (a)	(1036–4928) (d)	(62–4640) (b)	(19–4878) (e)	(140–4799) (a)	(946–4860) (d)
SST_{skin} (°C)	7.8 ± 0.2 (a,b)	9.1 ± 0.2 (a)	13.1 ± 0.1 (c)	17.7 ± 0.2 (d)	7.1 ± 0.2 (b)	10.9 ± 0.2 (e)	11.1 ± 0.1 (e)	16.6 ± 0.2 (d)
MSL pressure (hPa)	1009 ± 0 (a)	1014 ± 0 (b)	1015 ± 0 (b)	1018 ± 0 (c)	1009 ± 0 (a)	1014 ± 0 (b)	1011 ± 0 (d)	1018 ± 0 (c)
$Wind_{u\text{-}component}$ ($m\,s^{-1}$)	2.2 ± 0.1 (a,b)	2.2 ± 0.0 (a,c)	2.7 ± 0.1 (d)	2.5 ± 0.1 (b,d,e)	2.1 ± 0.1 (a,e)	2.0 ± 0.0 (c)	3.0 ± 0.1 (f)	2.7 ± 0.1 (d)
$Wind_{v\text{-}component}$ ($m\,s^{-1}$)	0.5 ± 0.0 (a,b)	0.8 ± 0.0 (a,c)	0.7 ± 0.0 (c)	0.8 ± 0.0 (c)	0.4 ± 0.0 (b,d)	0.4 ± 0.1 (a,d)	1.2 ± 0.0 (e)	0.8 ± 0.0 (c)
Wave (°true)	201 ± 1 (a)	202 ± 2 (a)	238 ± 1 (b)	231 ± 1 (c,d)	196 ± 1 (a)	220 ± 2 (e)	230 ± 1 (c)	235 ± 1 (b,d)
Phytoplankton and meroplankton abundances								
Diatoms (cells L^{-1})	69.4 ± 2.7 (a)	96.0 ± 7.3 (b)	59.2 ± 2.2 (a)	23.1 ± 1.8 (c)	44.4 ± 2.8 (d)	63.5 ± 3.3 (a)	44.0 ± 2.9 (e)	19.2 ± 1.3 (c)
Dinoflagellates (cells L^{-1})	16.8 ± 0.9 (a)	44.4 ± 4.5 (b)	35.9 ± 1.5 (b)	10.4 ± 0.8 (a,c)	8.3 ± 0.6 (d)	25.7 ± 1.5 (e)	20.3 ± 1.4 (f)	9.4 ± 0.7 (c)
Fish larvae (ind. m^{-3})	0.2 ± 0.0 (a)	0.5 ± 0.0 (b)	0.2 ± 0.0 (a)	0.1 ± 0.0 (c)	0.1 ± 0.0 (c,d)	0.3 ± 0.0 (b)	0.2 ± 0.0 (a,d)	0.1 ± 0.0 (a,d)
Invertebr. larvae (ind. m^{-3})	10.5 ± 1.9 (a)	263.3 ± 34.5 (b)	35.5 ± 4.3 (c)	2.3 ± 0.6 (a,d)	4.5 ± 0.9 (e)	101.5 ± 8.7 (b)	2.2 ± 0.3 (a)	1.6 ± 0.2 (d)
Community-weighted mean (CWM) trait values								
DVM_{index}	0.23 ± 0.00 (a)	0.17 ± 0.00 (b)	0.23 ± 0.00 (a)	0.27 ± 0.01 (c)	0.32 ± 0.00 (d)	0.25 ± 0.01 (a,c)	0.50 ± 0.01 (e)	0.54 ± 0.00 (e)
Classic DVM	0.06 ± 0.00 (a)	0.01 ± 0.00 (b)	0.11 ± 0.00 (c)	0.20 ± 0.01 (d)	0.20 ± 0.01 (d)	0.13 ± 0.01 (c)	0.44 ± 0.01 (e)	0.51 ± 0.01 (e)
Reverse DVM	0.17 ± 0.00 (a)	0.16 ± 0.00 (a)	0.12 ± 0.00 (b)	0.07 ± 0.00 (c)	0.12 ± 0.00 (b)	0.12 ± 0.00 (b)	0.05 ± 0.00 (c)	0.02 ± 0.00 (d)
Body length (mm)	3.60 ± 0.02 (a)	2.37 ± 0.03 (b)	2.40 ± 0.02 (b)	2.45 ± 0.02 (b)	3.96 ± 0.03 (c)	2.48 ± 0.02 (b)	3.14 ± 0.03 (d)	2.67 ± 0.01 (e)

(Continues)

TABLE 1 | (Continued)

	Bioregions							
	Day				Night			
	A	B	C	D	E	F	G	H
Myelination	0.88 ± 0.01 (a)	0.28 ± 0.02 (b)	0.44 ± 0.01 (c)	0.65 ± 0.01 (d)	0.74 ± 0.01 (e)	0.34 ± 0.01 (b,f)	0.33 ± 0.01 (b)	0.40 ± 0.01 (f)
Free-spawning	0.95 ± 0.00 (a)	1.00 ± 0.00 (b)	0.97 ± 0.00 (c)	0.91 ± 0.01 (d)	0.86 ± 0.00 (e,f)	0.96 ± 0.00 (a,c)	0.89 ± 0.00 (e)	0.86 ± 0.00 (f)
Sac-spawning	0.05 ± 0.00 (a)	0.00 ± 0.00 (b)	0.03 ± 0.00 (c)	0.09 ± 0.01 (d)	0.14 ± 0.00 (e,f)	0.04 ± 0.00 (a,c)	0.11 ± 0.00 (e)	0.14 ± 0.00 (f)
Omnivore	0.95 ± 0.00 (a)	1.00 ± 0.00 (b)	0.97 ± 0.00 (c)	0.87 ± 0.01 (d)	0.87 ± 0.00 (e)	0.96 ± 0.00 (a)	0.91 ± 0.00 (d)	0.90 ± 0.00 (d,e)
Carnivore	0.05 ± 0.00 (a)	0.01 ± 0.00 (b)	0.03 ± 0.00 (c)	0.14 ± 0.01 (d)	0.14 ± 0.00 (d)	0.05 ± 0.00 (a)	0.11 ± 0.00 (d)	0.15 ± 0.00 (e)
Herbivore	0.83 ± 0.01 (a)	0.28 ± 0.02 (b,c)	0.42 ± 0.01 (d)	0.55 ± 0.01 (e)	0.61 ± 0.01 (e)	0.31 ± 0.01 (b)	0.22 ± 0.01 (c)	0.25 ± 0.01 (c)
Detritivore	0.00 ± 0.00 (a)	0.00 ± 0.00 (b,c)	0.01 ± 0.00 (c)	0.03 ± 0.00 (d)	0.00 ± 0.00 (b)	0.01 ± 0.00 (c)	0.01 ± 0.00 (c)	0.03 ± 0.00 (e)
Current-feeding	0.96 ± 0.00 (a)	0.98 ± 0.00 (b)	0.93 ± 0.00 (c)	0.98 ± 0.00 (b)	0.84 ± 0.01 (d)	0.88 ± 0.01 (e)	0.68 ± 0.01 (f)	0.92 ± 0.00 (c)
Cruise-feeding	0.04 ± 0.00 (a)	0.02 ± 0.00 (b)	0.07 ± 0.00 (c)	0.07 ± 0.01 (c)	0.16 ± 0.01 (d)	0.12 ± 0.01 (e)	0.33 ± 0.01 (f)	0.13 ± 0.00 (d)
Ambush-feeding	0.08 ± 0.00 (a)	0.30 ± 0.01 (b,c)	0.39 ± 0.01 (b)	0.11 ± 0.01 (d)	0.16 ± 0.00 (e)	0.29 ± 0.01 (c)	0.18 ± 0.01 (e)	0.08 ± 0.00 (a,d)

Note: Kruskal-Wallis tests indicate a significant difference (p value < 0.001) between bioregions for all variables. Identical letters indicate no significant difference between bioregions at p value < 0.05, based on Dunn's post hoc tests with Hochberg adjustment. Sample sizes per bioregion: A. 420; B. 83; C. 317; D. 197; E. 306; F. 194; G. 164; H. 298 grid cells. Ab, abundance; SST_{skin}, Sea surface skin temperature; MSL pressure, Mean sea level pressure; Invertebr. larvae, Invertebrate larvae.

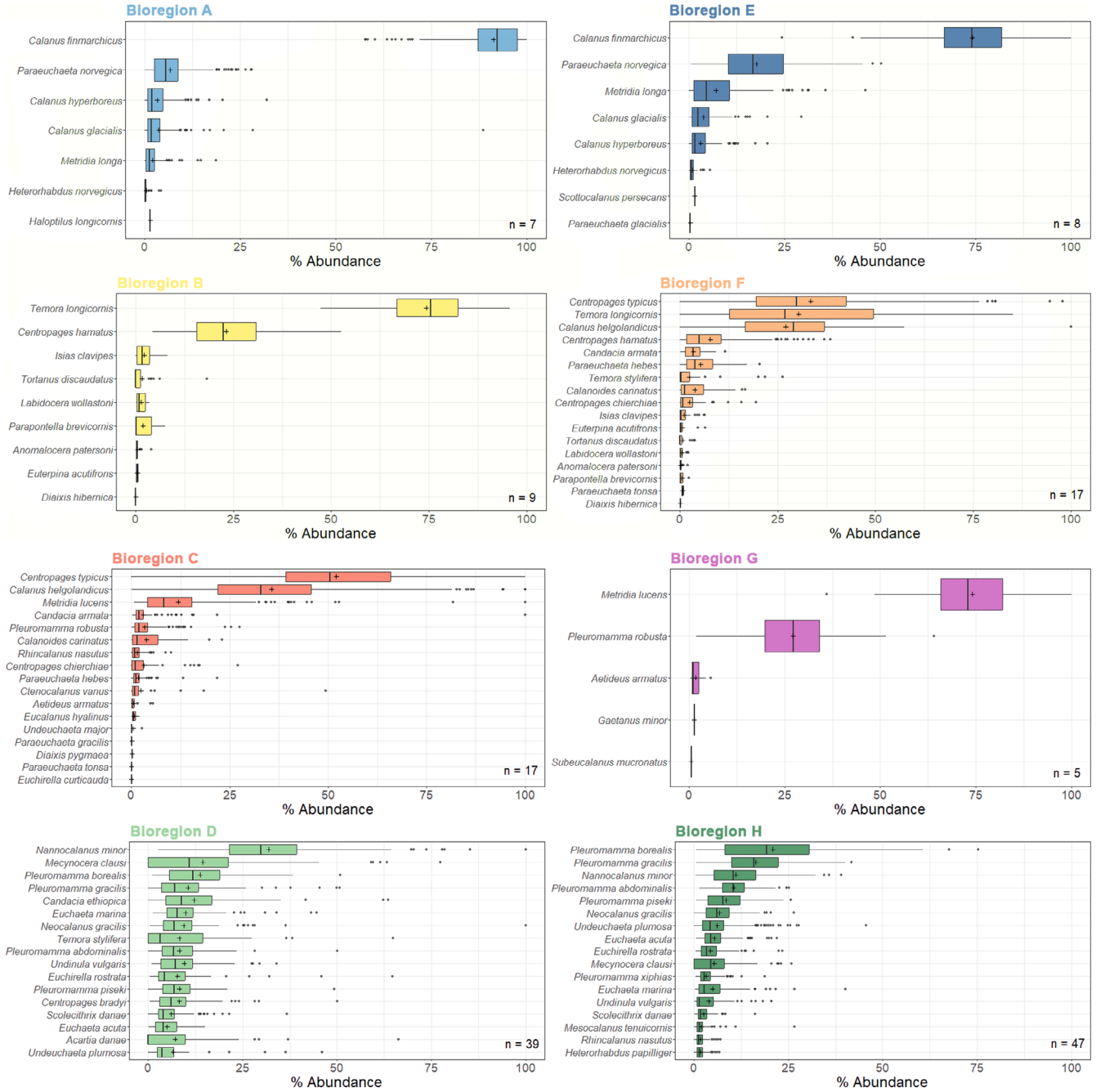

FIGURE 4 | Percentage of abundance of species in their affiliated bioregion during the day (left) and night (right). Species are ordered from the most to the least structuring, based on their codelength (= quantitative information from the Map Equation algorithm; the higher the codelength, the more structuring the species in its affiliated bioregion). Only the first 17 most structuring species of each bioregion are represented. The total number of structuring species in each bioregion is indicated in the bottom right-hand corners ($n = X$). The cross in the boxplot marks the mean of the distribution. Different colours indicate different bioregions (see Figure 3).

displaying a shallower depth range than bioregion F ($depth_{max}$ = 2083 m|$depth_{max}$ = 4878 m). Bioregion C (day) is characterised by warm-temperate waters (13.1°C ± 0.1°C) and relatively stable environmental conditions (negative part of axis 1 associated with lower standard deviations). This bioregion encompasses both a coastal and an open-ocean component (28–4872 m depth), with dominant coastal influence. At the centre of the CCA, bioregion G (night) appears as a transition zone between all other night bioregions.

3.3 | Copepod Diversity, Composition and CWM Traits in Bioregions

Dominant species in bioregions tend to be the most structuring, revealing two distinct profiles (Figure 4). No more than 25% of species significantly contribute to the structuring of bioregions A, B, C (day) and E, F, G (night), whereas this percentage rises to more than 60% in southern bioregions (D, H). The first group is characterised by the presence of a few dominant species

that significantly shape bioregions, while the second exhibits greater diversity and a more balanced influence on structuring. A North–South diversity gradient is observed in both day [Shannon's diversity = 0.4 (A) to 1.5 (D)] and night [Shannon's diversity = 0.7 (E) to 2.0 (H)] partitions, with the highest diversity at night (Table 1).

Northern bioregions (A|E) are structured by a few cold-water species (7|8 structuring species; Figure 4), which are relatively large (highest copepod community length, 3.60 ± 0.02 mm|3.96 ± 0.03 mm; Table 1) and tend towards herbivory (*Calanus finmarchicus*, *C. glacialis*, *C. hyperboreus*; Figure 3c). Moderate diel vertical migrations are observed (DVM_{index} = 0.23|0.32), with reverse DVM as the main pattern in bioregion A (0.17) and classic DVM as the main pattern in bioregion E (0.20). The strongly migratory species *Metridia longa* ranks as the third most structuring species of bioregion E (night; 7.1% ± 0.5%), whereas it represents 2.1% ± 0.2% of the abundance of bioregion A (day; Figure 4). Most species are myelinated, including *C. finmarchicus*, *C. glacialis*, *C. hyperboreus*, *Paraeuchaeta norvegica,* and *Paraeuchaeta glacialis* (present only at night; Figure 3c). *C. finmarchicus* plays a significant role in structuring bioregions A and E, representing on average 91.2% ± 0.4% (day) and 74.1% ± 0.7% (night) of the total abundance of the bioregion, followed by *P. norvegica* (6.8% ± 0.3%|17.7% ± 0.6%; Figure 4).

Southern bioregions (D|H) exhibit a diversity of warm-water species that contribute to their structuring (39|47 structuring species; Figure 4). In these diatom-poor open waters, detritivorous (e.g., *Euchirella* species, *Scaphocalanus echinatus*, *Scolecithrix danae*) and carnivorous (e.g., *Candacia*, *Paracandacia*, *Euchaeta,* and *Undeuchaeta* species) trophic groups emerge (Figure 3c). The main species demonstrate robust and classic DVM (e.g., *Euchirella* and *Pleuromamma* species, *Neocalanus gracilis*; Figure 3c). Such migratory species dominate at night (DVM_{index} = 0.27 for day, with 0.20 accounting for classic pattern and DVM_{index} = 0.54 for night, with 0.51 for classic pattern) and drive changes in the bioregion structure and composition between day (D) and night (H). Four *Pleuromamma* species rank among the top five most structuring species, representing more than 50% of the abundance of bioregion H (Figure 4), while bioregion D is primarily structured by *Nannocalanus minor* (31.9% ± 1.3%; also third most structuring species in bioregion H, representing 11.2% ± 0.4% of the total abundance) and *Mecynocera clausi* (14.5% ± 1.7%), then *Pleuromamma borealis* (13.7% ± 1.1%), *P. gracilis* (10.6% ± 1.0%), and *Candacia ethiopica* (12.1% ± 1.0%) (Figures 3b and 4).

The most striking day-night shifts in species composition are observed in the remaining bioregions. Bioregion C (day) occupies a central position in the North–South gradient and is structured by 17 species (Figure 4) with diverse thermal preferences, ranging from cold-temperate species (e.g., *Aetideus armatus*, *Metridia lucens,* and *Pleuromamma robusta*) to temperate species (e.g., *Calanus helgolandicus*, *Candacia armata*, *Centropages typicus,* and *Rhincalanus nasutus*) and warm-temperate/subtropical species (e.g., *Calanoides carinatus, Ctenocalanus vanus,* and *Undeuchaeta major*). Ambush-feeding species (*Aetideus armatus*, *Centropages chierchiae,* and *C. typicus*; Figure 3c) stand out in this bioregion where motile species (dinoflagellates, meroplankton) are rather highly abundant (Table 1). *C. typicus* accounts for 52.1% ± 1.2% on average of the abundance of the bioregion, followed by *C. helgolandicus* (35.6% ± 1.2%) and *M. lucens* (11.9% ± 0.7%) (Figure 4).

Bioregion C divides mostly into bioregion G and F at night (Figure 3b). Three dominant species of bioregion C mainly structure bioregion G (night), which is composed of 5 large cold-temperate and mixed-water species (Figure 4) with a free-spawning strategy, boasting the second-highest copepod community length after northern bioregions (3.14 ± 0.03 mm; Table 1). The two most structuring species, *Metridia lucens* (74.1% ± 1.0%) and *Pleuromamma robusta* (27.1% ± 0.9%), exhibit strong classic DVM patterns. The other three, *Aetideus armatus* (1.7% ± 0.2%), *Gaetanus minor* (1.3%), and *Subeucalanus mucronatus* (0.5%), are myelinated species, which help optimise their escape responses (the latter two also displaying strong DVM indexes; Appendix Figure S4). The three most structuring species of bioregion G are also abundant in neighbouring bioregions, especially in bioregion H, highlighting the transitional nature of bioregion G (Appendix Figure S5).

Continental shelf bioregion F (night) is structured by 17 species (Figure 4), including 7 warm-emperate/temperate pseudo-oceanic species from bioregion C (day) and a total of 9 shallow water/continental shelf species structuring bioregion B (day) (Figures 3b and 4). The latter is characterised by a strong inshore influence evidenced by high abundances of phytoplankton and meroplankton (Figure 3c, Table 1), therefore representing the most coastal part of bioregion F. This bioregion (B) is characterised by small to intermediate-sized species (smallest community body length of 2.37 ± 0.03 mm) such as the dominant *Temora longicornis* (representing on average 74.4% ± 1.2% of the abundance of the bioregion) and *Centropages hamatus* (23.1% ± 1.2%; Figure 4), along with *Isias clavipes*, *Parapontella brevicornis,* and *Tortanus discaudatus*. Copepods structuring this inshore-influenced area exhibit minimal DVM (DVM_{index} = 0.17), predominantly in reverse (0.16). These species are amyelinated, feed on a variety of prey (omnivory) and are free-spawning (except *Euterpina acutifrons*). The first most structuring species of bioregion F are alternately those of bioregions C and B: *C. typicus* (33.4% ± 1.4%), *T. longicornis* (30.3% ± 1.6%), *C. helgolandicus* (27.0% ± 1.2%), and *C. hamatus* (7.8% ± 0.7%) (Figure 4).

4 | Discussion

4.1 | Major Gradients Structure North Atlantic Partitions

This bioregionalisation study highlights two major gradients transcending diel variability and shaping North Atlantic partitions, similarly to what Longhurst (2007) observed for phytoplankton responses to external forcing (Reygondeau and Dunn 2019). Longitudinally, continental shelf bioregions (B|F) coincide with the 'coastal' biome and contrast with other bioregions further offshore. Latitudinally, we follow the previously described polar-temperate transition from northern (A|E) to southern bioregions (D|H). This North–South gradient extends beyond the pelagic domain, as it can even influence the bathyal benthos (Watling and Lapointe 2022). Such a strongly structuring gradient is allegedly linked to

temperature, with the 10°C isotherm associated with the oceanic polar front (Kléparski et al. 2021). The latter acts as a critical boundary for mesozooplankton distribution at the surface, as illustrated by the lowest participation coefficient values found at the extremities of the North–South gradient for both day and night conditions (Appendix Figure S6), although its influence weakens with depth (Vecchione et al. 2015). A latitudinal diversity gradient mirrors this biogeographic gradient. Southern communities, with higher diversity and functional redundancy, might be more stable over time and resilient to changes than northern communities (Biggs et al. 2020). All bioregions present higher diversity values at night than during the day, which is likely due to diel vertical migrations. Indeed, most migratory copepods dive into deeper waters during daytime and rise to surface waters during night-time (classic DVM; Bandara et al. 2021), which leads to greater aggregation (Wiebe et al. 2023) and can enhance diversity in nocturnal communities of the epipelagic zone (Govindarajan et al. 2023). The day/night consideration sheds light on a distinct bioregion (G), located at the bathymetric transition between the continental shelf of the British Isles and the Porcupine abyssal plain—associated with mixed and productive waters (Frigstad et al. 2015). In this region, Beaugrand et al. (2001) documented high variability in calanoid diversity, with strong nychthemeral cycles and seasonal fluctuations. This dynamic nature is supported by the presence of species exhibiting strong diel vertical migrations (e.g., *Metridia lucens*, *Pleuromamma robusta*), which are shared with the surrounding bioregions (i.e., high participation coefficient; Appendix Figure S6-right; Appendix Figure S5), reinforcing vertical and horizontal connectivity. In brief, our partitions reflect consistent macroscale environmental gradients while showing day/night discrepancies driven by changes in species composition mediated by diel vertical migration.

4.2 | About Trait–Environment Relationships

No statistically significant trait–environment relationship was detected at the study scale based on our approach. This could partly be explained by limitations in the trait dataset, which excludes intraspecific variations modulated by environmental factors (e.g., body size; Brun et al. 2016). Coupled with broad environmental data, the lack of intraspecific trait variability introduces uncertainties into community characterisation, resulting in a potentially biased representation of species traits at some locations (Albert et al. 2010). Nevertheless, community-weighted mean traits can reflect dominant structuring species traits displaying large-scale biogeographic patterns (Benedetti et al. 2023). In particular and qualitatively, community body length shows spatial patterns aligning with the detected environmental gradients. Northern bioregions (A|E) host large copepods. By contrast, southern bioregions (D|H) display a smaller community body length, and more inshore bioregions (B|C|F) have the smallest, echoing the findings of Brun et al. (2016) on similar data. These patterns support Bergmann's rule (1848), which stipulates that smaller species inhabit warmer waters (Campbell et al. 2021). Ectotherms tend to grow faster, with a higher moulting rate, and to reach maturity earlier, thus with a smaller body size, under warmer temperatures (Atkinson 1994; Miller et al. 1977). Roman and Pierson (2022) postulated that a smaller size could help copepods living in warmer coastal waters to adapt to the increased respiratory demand and reduced oxygen solubility (Verberk et al. 2011). Body size also influences predator–prey interactions (Hansen et al. 1994). Average zooplankton body size along the Atlantic Meridional Transect tends to decrease in oligotrophic seas dominated by pico- and nanoplankton and to increase in more nutrient-rich regions (San Martin et al. 2006). Predicted global warming-induced shifts in phytoplankton communities towards smaller cells (Henson et al. 2021) could lead to a decrease in average copepod body size through bottom-up effects, inducing shallower DVM (Ohman and Romagnan 2016) and reduced carbon export via the biological carbon pump (Bopp et al. 2005; Brun et al. 2019). Despite the above-mentioned limitations, community-weighted mean traits add a valuable functional component to the North Atlantic bioregionalisation, although further studies incorporating intraspecific trait variability and/or the arrival of new species will offer a more mechanistic understanding.

4.3 | Diel Vertical Migration Role in Community Dynamics and Trophic Interactions

DVM indirectly enhances aggregation (Chaput et al. 2019) as copepods tend not to migrate as compact populations (Roe 1984). Classic DVM (i.e., night-time ascent/daytime descent; Bandara et al. 2021) is strongest in southern (D|H) and transitional (G) bioregions, while northern bioregions (A|E) display a weaker reverse DVM (i.e., daytime ascent/night-time descent). DVM patterns closely relate to the structure of the pelagic food web, with predators adjusting their behavioural strategies in response to prey behaviour and *vice versa* (Pinti et al. 2019). Migrants' movements cause microscale turbulence (Kunze et al. 2006), making them extremely vulnerable to tactile predators (ambush-feeders; Bandara et al. 2021). Reverse DVM likely enables zooplankton to avoid non-visual invertebrate predators (e.g., chaetognaths, Saito and Kiørboe 2001) which exhibit classic DVM to escape their own visual predators (Ohman et al. 1983). Ambush-feeding copepods stand out in most inshore bioregions (B|C|F) with high prey concentrations (e.g., highest abundances of motile dinoflagellates), displaying weak reverse DVM or no DVM. In our study, ambush-feeders are often current-ambush feeders (i.e., mixed feeders), which aligns with the co-dominance pattern of mixed and active feeders in the northwestern European coasts observed by Brun et al. (2016). To complement this migration behaviour with greater responsiveness, copepods have evolved specialised escape mechanisms. *Metridia lucens* and *Pleuromamma robusta*, structuring transitional bioregion G and exhibiting large DVM amplitudes (Hays et al. 1995), use bioluminescence to evade visually sensitive predators in close proximity (Hartline et al. 1999). The other structuring copepods of bioregion G (*Aetideus armatus*, *Gaetanus minor,* and *Subeucalanus mucronatus*) have myelinated axons which enhance nerve impulse conduction, potentially inducing faster escape responses (Davis et al. 1999), although evidence remains debated (Waggett and Buskey 2008). Myelinated copepods dominate the structuring community of northern bioregions (A|E), while the most amyelinated community is found in coastal bioregions (B|F), in coherence with Brun et al. (2016). Myelination is thought to be more prevalent

where predation pressure and transparency are high, and food resources are low (Lenz 2012). This can seem counterintuitive, as myelination requires a large amount of dietary lipids to build cholesterol-rich membranes (Okamura et al. 1986), but it saves metabolic energy during copepod impulses (Hartline 2008; Ritchie 1984), which is particularly advantageous in low-food/high-quality conditions.

4.4 | Variability in DVM: Detection Limitations and Influence of Interrelated Traits

The timing and amplitude of DVM vary greatly, being highly dependent on copepods' depth of occurrence (Wiebe et al. 1992), and are influenced by several interrelated traits. At equivalent size, female krill migrate closer to the surface at night than males, probably due to the higher energetic demand for reproduction (Tarling 2003). Conversely, egg-carrying copepod females (sac-spawners) tend to remain deeper than egg-free individuals, minimising risk to offspring (Bollens and Frost 1991). Free-spawners' fecundity rates are significantly related to chlorophyll *a* concentration (Bunker and Hirst 2004), which helps to explain their dominance in phytoplankton-rich coastal bioregions (B|F). Osgood and Frost (1994) also suggested an ontogenetic effect, observing that older stages of *Calanus pacificus* are generally deeper than younger stages during the day. This may be linked to size (De Robertis et al. 2000), as we found that community body length was systematically greater at night. Sainmont et al. (2014) showed that small *Calanus* spp. exhibit clear DVM while large ones stay mostly at depth during the Greenland spring bloom.

Vertical migrations also vary seasonally, shifting between classic and reverse migrations, changing in periodicity and amplitude, or even ceasing entirely from one season to another (Bandara et al. 2016, 2021). This is particularly evident for large herbivorous-omnivorous copepods such as *Calanus finmarchicus*, *C. glacialis,* and *C. hyperboreus*, which structure northern bioregions (A|E) and experience highly seasonal climatic conditions and phytoplankton abundances (Barton et al. 2013). These high-latitude copepods tend to have particularly efficient lipid storage (Cavallo and Peck 2020) enabling them to overwinter by migrating to deeper waters, where they survive under a reduced metabolism thanks to their accumulated lipid reserves (Barton et al. 2013). This phenological behaviour induces a high seasonal variability in their vertical migrations (Krumhansl et al. 2018). Omnivorous (e.g., *Metridia longa*) and carnivorous (e.g., *Paraeuchaeta norvegica*) copepods are less subject to seasonal food shortages at high latitudes, since they may rely less on phytoplankton seasonality. Therefore, they do not usually exhibit such specific seasonal adaptations (Hagen and Auel 2001). In line with McGinty et al. (2018), carnivorous and detritivorous species are mostly found in warmer and less diatom-productive southern bioregions (D|H). In such regions, two trophic pathways may co-exist: *(i)* carnivorous species (Woodd-Walker et al. 2002) preying on smaller zooplankton or even larger gelatinous zooplankton (Takahashi et al. 2013) may exert top-down control on mesozooplankton, whereas *(ii)* detritivorous species feeding on marine snow aggregates and copepod carcasses contribute to organic matter recycling (Yamaguchi et al. 2002) and favour regenerated production (Becker et al. 2021).

The influence of interrelated traits on vertical migration depends on the species, their environment, and spatio-temporal scales. Disentangling the complex relationships between traits remains a challenge to gain insight into the ecological and functional consequences of vertical migration variability on ecosystems.

4.5 | Towards Dynamic Bioregions Highlighting Connectivity

While the same core structure and species composition as previous North Atlantic bioregionalisations have been found (Beaugrand et al. 2019; Kléparski et al. 2021), our partitions differ in terms of transitions between bioregions. We found bioregions with diffuse boundaries (high participation coefficients overall; Appendix Figure S6), indicating the connectivity of pelagic bioregions and suggesting that species can persist over a wide range of environmental variations (Woolley et al. 2020; Appendix Figure S5). This questions the ecological relevance of the greater number of bioregions with geometrically sharp transitions found in environment-based bioregionalisations (Morrone 2015). Transition zones are ecologically fascinating areas hosting intermixing communities and exhibiting high diversity (Hermogenes De Mendonça and Ebach 2020). They are inherently dynamic, with periods of stability and expansion (Lenoir et al. 2020). Range-edge individuals display phenotypic plasticity, adapting to environmental changes within a few generations (Pfennig 2021). Transition zones are thus particularly interesting to track biogeographic changes such as climate-driven shifts (e.g., North Atlantic regime shift; Beaugrand et al. 2008). A focus on seasonal dynamics could provide valuable insights into bioregions' variations and transitions over time, particularly in coastal and northernmost regions, where environmental conditions display strong seasonality. This could inform a typology of pelagic habitats that better reflects ecological reality, supporting ecosystem management (Holland et al. 2023). Ultimately, it is all about bringing species ecology back to the core of bioregionalisation studies by considering the behaviour and variability inherent to living organisms in a more dynamic partitioning to better reflect the functioning of pelagic ecosystems.

Author Contributions

M.V., E.G., D.V. and F.O. conceived the ideas and outlined the paper; M.V. analysed the data and led the writing with the assistance of E.G., D.V., F.B. and F.O. All authors wrote and/or contributed to the different sections of the manuscript based on their expertise.

Acknowledgements

This work was granted access to the HPC resources of the MeSU platform at Sorbonne Université. We thank the SACADO team, and particularly Nicolas Benoît for his assistance in optimising scripts and computation times. We would also like to thank Boris Leroy (BOREA, MNHN) for his advice on the network clustering approach, Pierre Hélaouët (Marine Biological Association of the U.K.) for his help in accessing and interpreting CPR data, Maria Grazia Mazzocchi (Stazione Zoologica Anton Dohrn) for her valuable suggestions in revising the paper, and Lucie Pellottiero (lucie.pellottiero@gmail.com) for her help with the graphic design. This study relies on CPR data from the Marine Biological Association in Plymouth and did not

involve any new fieldwork requiring specific permits or authorisations. The authors are grateful to all past and present members and supporters of the CPR Survey, whose dedicated efforts have been instrumental in establishing and maintaining the long-term CPR dataset. The Survey owes its existence to the owners, captains, and crews of the vessels responsible for towing the CPRs. This work was funded by the French Ministry of Ecological Transition, Biodiversity, Forest, Sea and Fisheries under the Direction Eau Biodiversité (DEB)—Muséum National d'Histoire Naturelle (MNHN) agreement relating to Descriptor 1 Biodiversity—Pelagic Habitats of the Marine Strategy Framework Directive (MSFD).

Conflicts of Interest

The authors declare no conflicts of interest.

Data Availability Statement

All data used in this study are available from the references indicated and the links below.

Copernicus ERA5 Data: https://cds.climate.copernicus.eu/datasets/reanalysis-era5-single-levels?tab=overview.

GEBCO Grid: https://www.bodc.ac.uk/data/published_data_library/catalogue/10.5285/e0f0bb80-ab44-2739-e053-6c86abc0289c/.

CPR Data are available on request from the Marine Biological Association (MBA), Plymouth. Details on the data request process can be found at https://www.cprsurvey.org/data/our-data/.

The trait dataset is available as Supplementary Appendix S2 in Benedetti et al. (2023): https://doi.org/10.1111/jbi.14512.

References

Albert, C. H., W. Thuiller, N. G. Yoccoz, R. Douzet, S. Aubert, and S. Lavorel. 2010. "A Multi-Trait Approach Reveals the Structure and the Relative Importance of Intra- vs. Interspecific Variability in Plant Traits." *Functional Ecology* 24, no. 6: 1192–1201. https://doi.org/10.1111/j.1365-2435.2010.01727.x.

Atkinson, D. 1994. "Temperature and Organism Size—A Biological law for Ectotherms?" *Advances in Ecological Research* 25: 1–58.

Bandara, K., Ø. Varpe, J. Søreide, J. Wallenschus, J. Berge, and K. Eiane. 2016. "Seasonal Vertical Strategies in a High-Arctic Coastal Zooplankton Community." *Marine Ecology Progress Series* 555: 49–64. https://doi.org/10.3354/meps11831.

Bandara, K., Ø. Varpe, L. Wijewardene, V. Tverberg, and K. Eiane. 2021. "Two Hundred Years of Zooplankton Vertical Migration Research." *Biological Reviews* 96, no. 4: 1547–1589. https://doi.org/10.1111/brv.12715.

Barton, A. D., A. J. Pershing, E. Litchman, et al. 2013. "The Biogeography of Marine Plankton Traits." *Ecology Letters* 16, no. 4: 522–534. https://doi.org/10.1111/ele.12063.

Batchelder, H. P., C. A. Edwards, and T. M. Powell. 2002. "Individual-Based Models of Copepod Populations in Coastal Upwelling Regions: Implications of Physiologically and Environmentally Influenced Diel Vertical Migration on Demographic Success and Nearshore Retention." *Progress in Oceanography* 53, no. 2–4: 307–333. https://doi.org/10.1016/S0079-6611(02)00035-6.

Batten, S. D., R. Clark, J. Flinkman, et al. 2003. "CPR Sampling: The Technical Background, Materials and Methods, Consistency and Comparability." *Progress in Oceanography* 58, no. 2–4: 193–215. https://doi.org/10.1016/j.pocean.2003.08.004.

Beaugrand, G. 2004. "The North Sea Regime Shift: Evidence, Causes, Mechanisms and Consequences." *Progress in Oceanography* 60, no. 2–4: 245–262. https://doi.org/10.1016/j.pocean.2004.02.018.

Beaugrand, G., M. Edwards, K. Brander, C. Luczak, and F. Ibanez. 2008. "Causes and Projections of Abrupt Climate-Driven Ecosystem Shifts in the North Atlantic: Causes and Projections of Abrupt Climate-Driven Ecosystem Shifts." *Ecology Letters* 11, no. 11: 1157–1168. https://doi.org/10.1111/j.1461-0248.2008.01218.x.

Beaugrand, G., M. Edwards, and P. Hélaouët. 2019. "An Ecological Partition of the Atlantic Ocean and its Adjacent Seas." *Progress in Oceanography* 173: 86–102. https://doi.org/10.1016/j.pocean.2019.02.014.

Beaugrand, G., and F. Ibanez. 2004. "Monitoring Marine Plankton Ecosystems. II: Long-Term Changes in North Sea Calanoid Copepods in Relation to Hydro-Climatic Variability." *Marine Ecology Progress Series* 284: 35–47. https://doi.org/10.3354/meps284035.

Beaugrand, G., F. Ibañez, and J. Lindley. 2001. "Geographical Distribution and Seasonal and Diel Changes in the Diversity of Calanoid Copepods in the North Atlantic and North Sea." *Marine Ecology Progress Series* 219: 189–203. https://doi.org/10.3354/meps219189.

Becker, É. C., M. G. Mazzocchi, L. C. P. De Macedo-Soares, M. Costa Brandão, and A. Santarosa Freire. 2021. "Latitudinal Gradient of Copepod Functional Diversity in the South Atlantic Ocean." *Progress in Oceanography* 199, no. 102: 710. https://doi.org/10.1016/j.pocean.2021.102710.

Benedetti, F., J. Wydler, and M. Vogt. 2023. "Copepod Functional Traits and Groups Show Divergent Biogeographies in the Global Ocean." *Journal of Biogeography* 50, no. 1: 8–22. https://doi.org/10.1111/jbi.14512.

Bergmann, C. 1848. *Ueber Die Verhältnisse Der Wärmeökonomie Der Tiere Zu Ihrer Grösse*. Vandenhoeck und Ruprecht.

Biggs, C. R., L. A. Yeager, D. G. Bolser, et al. 2020. "Does Functional Redundancy Affect Ecological Stability and Resilience?" *A Review and Meta-Analysis. Ecosphere* 11, no. 7: e03184. https://doi.org/10.1002/ecs2.3184.

Bloomfield, N. J., N. Knerr, and F. Encinas-Viso. 2018. "A Comparison of Network and Clustering Methods to Detect Biogeographical Regions." *Ecography* 41, no. 1: 1–10. https://doi.org/10.1111/ecog.02596.

Bohlin, L., D. Edler, A. Lancichinetti, and M. Rosvall. 2014. "Community Detection and Visualisation of Networks With the Map Equation Framework." In *Measuring Scholarly Impact*, edited by Y. Ding, R. Rousseau, and D. Wolfram, 3–34. Springer International Publishing. https://doi.org/10.1007/978-3-319-10,377-8_1.

Bollens, S. M., and B. W. Frost. 1991. "Ovigerity, Selective Predation, and Variable Diel Vertical Migration in *Euchaeta Elongata* (Copepoda: Calanoida)." *Oecologia* 87, no. 2: 155–161. https://doi.org/10.1007/BF00325252.

Bollens, S. M., G. Rollwagen-Bollens, J. A. Quenette, and A. B. Bochdansky. 2011. "Cascading Migrations and Implications for Vertical Fluxes in Pelagic Ecosystems." *Journal of Plankton Research* 33, no. 3: 349–355. https://doi.org/10.1093/plankt/fbq152.

Bopp, L., O. Aumont, P. Cadule, S. Alvain, and M. Gehlen. 2005. "Response of Diatoms Distribution to Global Warming and Potential Implications: A Global Model Study." *Geophysical Research Letters* 32, no. 19: 23653. https://doi.org/10.1029/2005GL023653.

Boudinot, F. G., and J. Wilson. 2020. "Does a Proxy Measure up? A Framework to Assess and Convey Proxy Reliability." *Climate of the Past* 16, no. 5: 1807–1820. https://doi.org/10.5194/cp-16-1807-2020.

Bruelheide, H., J. Dengler, O. Purschke, et al. 2018. "Global Trait–Environment Relationships of Plant Communities." *Nature Ecology & Evolution* 2, no. 12: 1906–1917. https://doi.org/10.1038/s41559-018-0699-8.

Brun, P., M. R. Payne, and T. Kiørboe. 2016. "Trait Biogeography of Marine Copepods—An Analysis Across Scales." *Ecology Letters* 19, no. 12: 1403–1413. https://doi.org/10.1111/ele.12688.

Brun, P., K. Stamieszkin, A. W. Visser, P. Licandro, M. R. Payne, and T. Kiørboe. 2019. "Climate Change has Altered Zooplankton-Fuelled Carbon Export in the North Atlantic." *Nature Ecology & Evolution* 3, no. 3: 416–423. https://doi.org/10.1038/s41559-018-0780-3.

Bunker, A., and A. Hirst. 2004. "Fecundity of Marine Planktonic Copepods: Global Rates and Patterns in Relation to Chlorophyll a, Temperature, and Body Weight." *Marine Ecology Progress Series* 279: 161–181. https://doi.org/10.3354/meps279161.

Campbell, M. D., D. S. Schoeman, W. Venables, et al. 2021. "Testing Bergmann's Rule in Marine Copepods." *Ecography* 44, no. 9: 1283–1295. https://doi.org/10.1111/ecog.05545.

Cavallo, A., and L. S. Peck. 2020. "Lipid Storage Patterns in Marine Copepods: Environmental, Ecological, and Intrinsic Drivers." *ICES Journal of Marine Science* 77, no. 5: 1589–1601. https://doi.org/10.1093/icesjms/fsaa070.

Chaput, R., J. E. Majoris, P. M. Buston, and C. B. Paris. 2019. "Hydrodynamic and Biological Constraints on Group Cohesion in Plankton." *Journal of Theoretical Biology* 482, no. 109: 987. https://doi.org/10.1016/j.jtbi.2019.08.018.

Conroy, J. A., D. K. Steinberg, P. S. Thibodeau, and O. Schofield. 2020. "Zooplankton Diel Vertical Migration During Antarctic Summer." *Deep Sea Research Part I: Oceanographic Research Papers* 162, no. 103: 324. https://doi.org/10.1016/j.dsr.2020.103324.

Davis, A. D., T. M. Weatherby, D. K. Hartline, and P. H. Lenz. 1999. "Myelin-Like Sheaths in Copepod Axons." *Nature* 398: 571. https://doi.org/10.1038/19212.

De Robertis, A., J. S. Jaffe, and M. D. Ohman. 2000. "Size-Dependent Visual Predation Risk and the Timing of Vertical Migration in Zooplankton." *Limnology and Oceanography* 45, no. 8: 1838–1844. https://doi.org/10.4319/lo.2000.45.8.1838.

Djeghri, N., A. Boyé, C. Ostle, and P. Hélaouët. 2023. "Reinterpreting two Regime Shifts in North Sea Plankton Communities Through the Lens of Functional Traits." *Global Ecology and Biogeography* 32, no. 6: 962–975. https://doi.org/10.1111/geb.13659.

Edler, D., T. Guedes, A. Zizka, M. Rosvall, and A. Antonelli. 2016. "Infomap Bioregions: Interactive Mapping of Biogeographical Regions From Species Distributions." *Systematic Biology* 66, no. 2: 197–204. https://doi.org/10.1093/sysbio/syw087.

Ferrari, A., D. Janisch Alvares, P. M. Buratto, and K. Ribeiro Barão. 2022. "Distribution Patterns of Triatominae (Hemiptera: Reduviidae) in the Americas: An Analysis Based on Networks and Endemicity." *Cladistics* 38, no. 5: 563–581. https://doi.org/10.1111/cla.12500.

Frigstad, H., S. A. Henson, S. E. Hartman, et al. 2015. "Links Between Surface Productivity and Deep Ocean Particle Flux at the Porcupine Abyssal Plain Sustained Observatory." *Biogeosciences* 12, no. 19: 5885–5897. https://doi.org/10.5194/bg-12-5885-2015.

GEBCO Compilation Group. 2022. "GEBCO 2022 Grid." [Dataset]. https://doi.org/10.5285/e0f0bb80-ab44-2739-e053-6c86abc0289c.

Goberville, E., G. Beaugrand, and M. Edwards. 2014. "Synchronous Response of Marine Plankton Ecosystems to Climate in the Northeast Atlantic and the North Sea." *Journal of Marine Systems* 129: 189–202. https://doi.org/10.1016/j.jmarsys.2013.05.008.

Govindarajan, A. F., J. K. Llopiz, P. E. Caiger, et al. 2023. "Assessing Mesopelagic Fish Diversity and Diel Vertical Migration With Environmental DNA." *Frontiers in Marine Science* 10: 1219993. https://doi.org/10.3389/fmars.2023.1219993.

Hagen, W., and H. Auel. 2001. "Seasonal Adaptations and the Role of Lipids in Oceanic Zooplankton." *Zoology* 104, no. 3–4: 313–326. https://doi.org/10.1078/0944-2006-00037.

Hansen, B., P. K. Bjornsen, and P. J. Hansen. 1994. "The Size Ratio Between Planktonic Predators and Their Prey." *Limnology and Oceanography* 39, no. 2: 395–403. https://doi.org/10.4319/lo.1994.39.2.0395.

Hardy, A. C. 1939. "Ecological Investigations With the Continuous Plankton Recorder: Object, Plan, and Methods." *Hull Bulletins of Marine Ecology* 1: 1–57.

Hartline, D. K. 2008. "What is Myelin?" *Neuron Glia Biology* 4, no. 2: 153–163. https://doi.org/10.1017/S1740925X09990263.

Hartline, D. K., E. J. Buskey, and P. H. Lenz. 1999. "Rapid Jumps and Bioluminescence Elicited by Controlled Hydrodynamic Stimuli in a Mesopelagic Copepod *Pleuromamma xiphias*." *Biological Bulletin* 197, no. 2: 132–143. https://doi.org/10.2307/1542610.

Hays, G. C., A. J. Warner, and C. A. Proctor. 1995. "Spatio-Temporal Patterns in the Diel Vertical Migration of the Copepod *Metridia Lucens* in the Northeast Atlantic Derived From the Continuous Plankton Recorder Survey." *Limnology and Oceanography* 40, no. 3: 469–475. https://doi.org/10.4319/lo.1995.40.3.0469.

Hébert, M.-P., and B. E. Beisner. 2020. "Functional Trait Approaches for the Study of Metazooplankton Ecology." In *Zooplankton Ecology*, 3–27. CRC Press.

Hélaouët, P., G. Beaugrand, and G. Reygondeau. 2016. "Reliability of Spatial and Temporal Patterns of *C. finmarchicus* Inferred From the CPR Survey." *Journal of Marine Systems* 153: 18–24. https://doi.org/10.1016/j.jmarsys.2015.09.001.

Henson, S. A., B. B. Cael, S. R. Allen, and S. Dutkiewicz. 2021. "Future Phytoplankton Diversity in a Changing Climate." *Nature Communications* 12, no. 1: 5372. https://doi.org/10.1038/s41467-021-25,699-w.

Hermogenes De Mendonça, L., and M. C. Ebach. 2020. "A Review of Transition Zones in Biogeographical Classification." *Biological Journal of the Linnean Society* 131, no. 4: 717–736. https://doi.org/10.1093/biolinnean/blaa120.

Hersbach, H., B. Bell, P. Berrisford, et al. 2023. "ERA5 Hourly Data on Single Levels From 1940 to Present." *Copernicus Climate Change Service (C3S) Climate Data Store (CDS)*. [Dataset]. https://doi.org/10.24381/cds.adbb2d47.

Holland, M. M., A. Louchart, L. F. Artigas, et al. 2023. "Major Declines in NE Atlantic Plankton Contrast With More Stable Populations in the Rapidly Warming North Sea." *Science of the Total Environment* 898, no. 165: 505. https://doi.org/10.1016/j.Scitotenv.2023.165505.

Irigoien, X., D. Conway, and R. Harris. 2004. "Flexible Diel Vertical Migration Behaviour of Zooplankton in the Irish Sea." *Marine Ecology Progress Series* 267: 85–97. https://doi.org/10.3354/meps267085.

Kassambara, A. 2023. "*rstatix: Pipe-Friendly Framework for Basic Statistical Tests* (0.7.2)." https://cran.r-project.org/package=rstatix.

Katija, K., and J. O. Dabiri. 2009. "A Viscosity-Enhanced Mechanism for Biogenic Ocean Mixing." *Nature* 460, no. 7255: 624–626. https://doi.org/10.1038/nature08207.

Kléparski, L., G. Beaugrand, and M. Edwards. 2021. "Plankton Biogeography in the North Atlantic Ocean and its Adjacent Seas: Species Assemblages and Environmental Signatures." *Ecology and Evolution* 11, no. 10: 5135–5149. https://doi.org/10.1002/ece3.7406.

Koblick, D. 2023. "*SolarAzEl: Vectorized Solar Azimuth and Elevation Estimation* (1.1.0.0)." https://www.mathworks.com/matlabcentral/fileexchange/23051-vectorized-solar-azimuth-and-elevation-estimation.

Krumhansl, K. A., E. J. H. Head, P. Pepin, et al. 2018. "Environmental Drivers of Vertical Distribution in Diapausing Calanus Copepods in the Northwest Atlantic." *Progress in Oceanography* 162: 202–222. https://doi.org/10.1016/j.Pocean.2018.02.018.

Kunze, E., J. F. Dower, I. Beveridge, R. Dewey, and K. P. Bartlett. 2006. "Observations of Biologically Generated Turbulence in a Coastal Inlet."

Science 313, no. 5794: 1768–1770. https://doi.org/10.1126/Science.1129378.

Lagonigro, R., R. Oller, and J. Martori. 2023. "*AQuadtree: Confidentiality of Spatial Point Data* (1.0.4)." https://CRAN.R-project.org/package=AQuadtree.

Lenoir, J., R. Bertrand, L. Comte, et al. 2020. "Species Better Track Climate Warming in the Oceans Than on Land." *Nature Ecology & Evolution* 4, no. 8: 1044–1059. https://doi.org/10.1038/s41559-020-1198-2.

Lenz, P. H. 2012. "The Biogeography and Ecology of Myelin in Marine Copepods." *Journal of Plankton Research* 34, no. 7: 575–589. https://doi.org/10.1093/plankt/fbs037.

Leroy, B. 2024. "*biogeonetworks: Biogeographical Network Manipulation and Analysis* (0.1.2)." https://github.com/Farewe/biogeonetworks.

Leroy, B., C. Bellard, M. S. Dias, et al. 2023. "Major Shifts in Biogeographic Regions of Freshwater Fishes as Evidence of the Anthropocene Epoch." *Science Advances* 9, no. 46: eadi5502. https://doi.org/10.1126/sciadv.adi5502.

Leroy, B., M. S. Dias, E. Giraud, et al. 2019. "Global Biogeographical Regions of Freshwater Fish Species." *Journal of Biogeography* 46, no. 11: 2407–2419. https://doi.org/10.1111/jbi.13674.

Lewis, J. R. 1964. *The Ecology of Rocky Shores*. 1st ed. English Universities Press.

Lewis, K., J. I. Allen, A. J. Richardson, and J. T. Holt. 2006. "Error Quantification of a High-Resolution Coupled Hydrodynamic-Ecosystem Coastal-Ocean Model: Part3, Validation With Continuous Plankton Recorder Data." *Journal of Marine Systems* 63, no. 3–4: 209–224. https://doi.org/10.1016/j.jmarsys.2006.08.001.

Litchman, E., M. D. Ohman, and T. Kiørboe. 2013. "Trait-Based Approaches to Zooplankton Communities." *Journal of Plankton Research* 35, no. 3: 473–484. https://doi.org/10.1093/plankt/fbt019.

Longhurst, A. R. 2007. *Ecological Geography of the Sea*. 2nd ed. Academic Press.

Marine Biological Association of the UK (MBA). 2022. "CPR Data request Eric Goberville Sorbonne University June 2022." *The Archive for Marine Species and Habitats Data (DASSH)*. [Dataset]. https://doi.dassh.ac.uk/data/1842.

McGinty, N., A. Barton, N. Record, Z. Finkel, and A. Irwin. 2018. "Traits Structure Copepod Niches in the North Atlantic and Southern Ocean." *Marine Ecology Progress Series* 601: 109–126. https://doi.org/10.3354/meps12660.

McQuatters-Gollop, A., D. Raitsos, M. Edwards, and M. Attrill. 2007. "Spatial Patterns of Diatom and Dinoflagellate Seasonal Cycles in the NE Atlantic Ocean." *Marine Ecology Progress Series* 339: 301–306. https://doi.org/10.3354/meps339301.

Miller, C. B., J. K. Johnson, and D. R. Heinle. 1977. "Growth Rules in the Marine Copepod Genus *Acartia*." *Limnology and Oceanography* 22, no. 2: 326–335. https://doi.org/10.4319/lo.1977.22.2.0326.

Morrone, J. J. 2015. "Biogeographical Regionalisation of the World: A Reappraisal." *Australian Systematic Botany* 28, no. 3: 81. https://doi.org/10.1071/SB14042.

Munk, P. 1997. "Prey Size Spectra and Prey Availability of Larval and Small Juvenile Cod." *Journal of Fish Biology* 51, no. sA: 340–351. https://doi.org/10.1111/j.1095-8649.1997.tb06107.x.

Ohman, M. D. 1990. "The Demographic Benefits of Diel Vertical Migration by Zooplankton." *Ecological Monographs* 60, no. 3: 257–281. https://doi.org/10.2307/1943058.

Ohman, M. D., B. W. Frost, and E. B. Cohen. 1983. "Reverse Diel Vertical Migration: An Escape From Invertebrate Predators." *Science* 220, no. 4604: 1404–1407. https://doi.org/10.1126/science.220.4604.1404.

Ohman, M. D., and J. Romagnan. 2016. "Nonlinear Effects of Body Size and Optical Attenuation on Diel Vertical Migration by Zooplankton." *Limnology and Oceanography* 61, no. 2: 765–770. https://doi.org/10.1002/lno.10251.

Okamura, N., H. Yamaguchi, M. Stoskopf, Y. Kishimoto, and T. Saida. 1986. "Isolation and Characterisation of Multilayered Sheath Membrane Rich in Glucocerebroside From Shrimp Ventral Nerve." *Journal of Neurochemistry* 47, no. 4: 1111–1116. https://doi.org/10.1111/j.1471-4159.1986.tb00728.x.

Oksanen, J., G. Simpson, F. Blanchet, et al. 2022. "*vegan: Community Ecology Package* (2.6.4)." https://CRAN.R-project.org/package=vegan.

Osgood, K., and B. Frost. 1994. "Ontogenetic Diel Vertical Migration Behaviours of the Marine Planktonic Copepods *Calanus pacificus* and *Metridia lucens*." *Marine Ecology Progress Series* 104: 13–25. https://doi.org/10.3354/meps104013.

Pata, P. R., M. Galbraith, K. Young, A. R. Margolin, R. I. Perry, and B. P. V. Hunt. 2022. "Persistent Zooplankton Bioregions Reflect Long-Term Consistency of Community Composition and Oceanographic Drivers in the NE Pacific." *Progress in Oceanography* 206, no. 102: 849. https://doi.org/10.1016/j.pocean.2022.102849.

Pfennig, D. W. 2021. "Key Questions About Phenotypic Plasticity." In *Phenotypic Plasticity & Evolution*, edited by D. W. In, 1st ed., 55–88. CRC Press. https://doi.org/10.1201/9780429343001-4.

Pinti, J., T. DeVries, T. Norin, et al. 2023. "Model Estimates of Metazoans' Contributions to the Biological Carbon Pump." *Biogeosciences* 20, no. 5: 997–1009. https://doi.org/10.5194/bg-20-997-2023.

Pinti, J., T. Kiørboe, U. H. Thygesen, and A. W. Visser. 2019. "Trophic Interactions Drive the Emergence of Diel Vertical Migration Patterns: A Game-Theoretic Model of Copepod Communities." *Proceedings of the Royal Society B: Biological Sciences* 286, no. 1911: 645. https://doi.org/10.1098/rspb.2019.1645.

R Core Team. 2023. *R: A Language and Environment for Statistical Computing (4.3.2)*. R Foundation for Statistical Computing. https://www.R-project.org/.

Ratnarajah, L., R. Abu-Alhaija, A. Atkinson, et al. 2023. "Monitoring and Modelling Marine Zooplankton in a Changing Climate." *Nature Communications* 14, no. 1: 564. https://doi.org/10.1038/s41467-023-36,241-5.

Razouls, C., N. Desreumaux, J. Kouwenberg, and F. de Bovée. 2005–2024. *Biodiversity of Marine Planktonic Copepods (Morphology, Geographical Distribution and Biological Data)*. Sorbonne University. http://copepodes.obs-banyuls.fr/en.

Record, N. R., R. Ji, F. Maps, et al. 2018. "Copepod Diapause and the Biogeography of the Marine Lipidscape." *Journal of Biogeography* 45, no. 10: 2238–2251. https://doi.org/10.1111/jbi.13414.

Reid, P. C., J. M. Colebrook, J. B. L. Matthews, and J. Aiken. 2003. "The Continuous Plankton Recorder: Concepts and History, From Plankton Indicator to Undulating Recorders." *Progress in Oceanography* 58, no. 2–4: 117–173. https://doi.org/10.1016/j.pocean.2003.08.002.

Reygondeau, G., and D. Dunn. 2019. "Pelagic Biogeography." In *Encyclopedia of Ocean Sciences*, 588–598. Elsevier. https://doi.org/10.1016/B978-0-12-409,548-9.11633-1.

Richardson, A. J., A. W. Walne, A. W. G. John, et al. 2006. "Using Continuous Plankton Recorder Data." *Progress in Oceanography* 68, no. 1: 27–74. https://doi.org/10.1016/j.pocean.2005.09.011.

Ritchie, J. M. 1984. "Physiological Basis of Conduction in Myelinated Nerve Fibres." In *Myelin*, 2nd ed., 117–145. Springer. https://doi.org/10.1007/978-1-4757-1830-0_4.

Roe, H. S. J. 1984. "The Diel Migrations and Distributions Within a Mesopelagic Community in the North East Atlantic. 4. The Copepods." *Progress in Oceanography* 13, no. 3–4: 353–388. https://doi.org/10.1016/0079-6611(84)90013-2.

Rojas, A., P. Patarroyo, L. Mao, P. Bengtson, and M. Kowalewski. 2017. "Global Biogeography of Albian Ammonoids: A Network-Based Approach." *Geology* 45, no. 7: 659–662. https://doi.org/10.1130/G38944.1.

Roman, M. R., and J. J. Pierson. 2022. "Interactive Effects of Increasing Temperature and Decreasing Oxygen on Coastal Copepods." *Biological Bulletin* 243, no. 2: 171–183. https://doi.org/10.1086/722111.

Rosvall, M., and C. T. Bergstrom. 2008. "Maps of Random Walks on Complex Networks Reveal Community Structure." *Proceedings of the National Academy of Sciences* 105, no. 4: 1118–1123. https://doi.org/10.1073/pnas.0706851105.

Sainmont, J., A. Gislason, J. Heuschele, et al. 2014. "Inter- and Intra-Specific Diurnal Habitat Selection of Zooplankton During the Spring Bloom Observed by Video Plankton Recorder." *Marine Biology* 161, no. 8: 1931–1941. https://doi.org/10.1007/s00227-014-2475-x.

Saito, H., and T. Kiørboe. 2001. "Feeding Rates in the Chaetognath *Sagitta elegans*: Effects of Prey Size, Prey Swimming Behaviour, and Small-Scale Turbulence." *Journal of Plankton Research* 23, no. 12: 1385–1398. https://doi.org/10.1093/plankt/23.12.1385.

San Martin, E., X. Irigoien, P. H. Roger, Â. L. Urrutia, M. V. Zubkov, and J. L. Heywood. 2006. "Variation in the Transfer of Energy in Marine Plankton Along a Productivity Gradient in the Atlantic Ocean." *Limnology and Oceanography* 51, no. 5: 2084–2091. https://doi.org/10.4319/lo.2006.51.5.2084.

Stamieszkin, K., A. J. Pershing, N. R. Record, C. H. Pilskaln, H. G. Dam, and L. R. Feinberg. 2015. "Size as the Master Trait in Modelled Copepod Faecal Pellet Carbon Flux." *Limnology and Oceanography* 60, no. 6: 2090–2107. https://doi.org/10.1002/lno.10156.

Strathmann, R. R. 1996. "Are Planktonic Larvae of Marine Benthic Invertebrates Too Scarce to Compete Within Species?" *Oceanologica Acta* 19, no. 3–4: 399–407.

Takahashi, K., T. Ichikawa, H. Saito, et al. 2013. "Sapphirinid Copepods as Predators of Doliolids: Their Role in Doliolid Mortality and Sinking Flux." *Limnology and Oceanography* 58, no. 6: 1972–1984. https://doi.org/10.4319/lo.2013.58.6.1972.

Tarling, G. 2003. "Sex-Dependent Diel Vertical Migration in Northern Krill *Meganyctiphanes norvegica* and its Consequences for Population Dynamics." *Marine Ecology Progress Series* 260: 173–188. https://doi.org/10.3354/meps260173.

Thygesen, U. H., and T. A. Patterson. 2019. "Oceanic Diel vertical Migrations Arising From a Predator–Prey Game." *Theoretical Ecology* 12, no. 1: 17–29. https://doi.org/10.1007/s12080-018-0385-0.

Turner, J. T. 2002. "Zooplankton Faecal Pellets, Marine Snow and Sinking Phytoplankton Blooms." *Aquatic Microbial Ecology* 27: 57–102. https://doi.org/10.3354/ame027057.

Turner, J. T. 2004. "The Importance of Small Planktonic Copepods and Their Roles in Pelagic Marine Food Webs." *Zoological Studies* 43, no. 2: 255–266.

Vecchione, M., T. Falkenhaug, T. Sutton, et al. 2015. "The Effect of the North Atlantic Subpolar Front as a Boundary in Pelagic Biogeography Decreases With Increasing Depth and Organism Size." *Progress in Oceanography* 138: 105–115. https://doi.org/10.1016/j.pocean.2015.08.006.

Verberk, W. C. E. P., D. T. Bilton, P. Calosi, and J. I. Spicer. 2011. "Oxygen Supply in Aquatic Ectotherms: Partial Pressure and Solubility Together Explain Biodiversity and Size Patterns." *Ecology* 92, no. 8: 1565–1572. https://doi.org/10.1890/10-2369.1.

Victorero, L., S. Samadi, T. D. O'Hara, et al. 2023. "Global Benthic Biogeographical Regions and Macroecological Drivers for Ophiuroids." *Ecography* 2023, no. 9: e06627. https://doi.org/10.1111/ecog.06627.

Vilhena, D. A., and A. Antonelli. 2015. "A Network Approach for Identifying and Delimiting Biogeographical Regions." *Nature Communications* 6, no. 1: 6848. https://doi.org/10.1038/ncomms7848.

Violle, C., M. Navas, D. Vile, et al. 2007. "Let the Concept of Trait be Functional!" *Oikos* 116, no. 5: 882–892. https://doi.org/10.1111/j.0030-1299.2007.15559.x.

Waggett, R. J., and E. J. Buskey. 2008. "Escape Reaction Performance of Myelinated and Non-Myelinated Calanoid Copepods." *Journal of Experimental Marine Biology and Ecology* 361, no. 2: 111–118. https://doi.org/10.1016/j.jembe.2008.05.006.

Watling, L., and A. Lapointe. 2022. "Global Biogeography of the Lower Bathyal (700–3000 m) as Determined From the Distributions of Cnidarian Anthozoans." *Deep Sea Research Part I: Oceanographic Research Papers* 181, no. 103: 703. https://doi.org/10.1016/j.dsr.2022.103703.

Wiebe, P. H., N. J. Copley, and S. H. Boyd. 1992. "Coarse-Scale Horizontal Patchiness and Vertical Migration of Zooplankton in Gulf Stream Warm-Core Ring 82-H." *Deep Sea Research Part A. Oceanographic Research Papers* 39: S247–S278. https://doi.org/10.1016/S0198-0149(11)80015-4.

Wiebe, P. H., A. C. Lavery, and G. L. Lawson. 2023. "Biogeographic Variations in Diel Vertical Migration Determined From Acoustic Backscattering in the Northwest Atlantic Ocean." *Deep Sea Research Part I: Oceanographic Research Papers* 193, no. 103: 887. https://doi.org/10.1016/j.dsr.2022.103887.

Williamson, C. E., J. M. Fischer, S. M. Bollens, E. P. Overholt, and J. K. Breckenridge. 2011. "Towards a More Comprehensive Theory of Zooplankton Diel Vertical Migration: Integrating Ultraviolet Radiation and Water Transparency Into the Biotic Paradigm." *Limnology and Oceanography* 56, no. 5: 1603–1623. https://doi.org/10.4319/lo.2011.56.5.1603.

Woodd-Walker, R., P. Ward, and A. Clarke. 2002. "Large-Scale Patterns in Diversity and Community Structure of Surface Water Copepods From the Atlantic Ocean." *Marine Ecology Progress Series* 236: 189–203. https://doi.org/10.3354/meps236189.

Woolley, S. N. C., S. D. Foster, N. J. Bax, et al. 2020. "Bioregions in Marine Environments: Combining Biological and Environmental Data for Management and Scientific Understanding." *BioScience* 70, no. 1: 48–59. https://doi.org/10.1093/biosci/biz133.

Yamaguchi, A., C. J. Ashjian, and R. G. Campbell. 2022. "Comparison of Population Structure, Vertical Distribution, and Growth of Sympatric, Carnivorous, Mesopelagic Copepods, *Paraeuchaeta glacialis* and *Heterorhabdus norvegicus*, in the Western Arctic Ocean." *Journal of Plankton Research* 44, no. 3: 443–453. https://doi.org/10.1093/plankt/fbac019.

Yamaguchi, A., Y. Watanabe, H. Ishida, et al. 2002. "Community and Trophic Structures of Pelagic Copepods Down to Greater Depths in the Western Subarctic Pacific (WEST-COSMIC)." *Deep Sea Research Part I: Oceanographic Research Papers* 49, no. 6: 1007–1025. https://doi.org/10.1016/S0967-0637(02)00008-0.

Zelený, D. 2018. "Which Results of the Standard Test for Community-Weighted Mean Approach Are Too Optimistic?" *Journal of Vegetation Science* 29, no. 6: 953–966. https://doi.org/10.1111/jvs.12688.

Zelený, D. 2021. "*weimea: Weighted Mean Analysis* (0.1.19)." https://r-forge.r-project.org/projects/weimea/.

Zelený, D., and A. P. Schaffers. 2012. "Too Good to Be True: Pitfalls of Using Mean Ellenberg Indicator Values in Vegetation Analyses." *Journal of Vegetation Science* 23, no. 3: 419–431. https://doi.org/10.1111/j.1654-1103.2011.01366.x.

Supporting Information

Additional supporting information can be found online in the Supporting Information section.